SHRP-ID/UFR-91-516

Prediction of Fatigue Cracking and Rutting in Asphalt Pavements by Small-Scale Centrifuge Models

Yang H. Huang
Vincent P. Drnevich
Hossien Roghani

Department of Civil Engineering
University of Kentucky
Lexington, Kentucky

Strategic Highway Research Program
National Research Council
Washington, D.C. 1991

SHRP-ID/UFR-91-516
Contract ID003
Project Manager: *Jack Youtcheff*

April 1991

key words:
centrifuge
centrifuge specimens
computer input
computer models
creep tests
cylindrical specimens
data acquisition systems
data reduction
repeated load tests
sand specimens
test capsule

Strategic Highway Research Program
2101 Constitution Avenue, N.W.
Washington,D.C. 20418

(202) 334-3774

Acknowledgments

The research described herein was supported by the Strategic Highway Research Program (SHRP). SHRP is a unit of the National Research Council that was authorized by section 128 of the Surface Transportation and Uniform Relocation Assistance Act of 1987.

Contents

List of Tables

List of Figures

Abstract

This study investigated the feasibility of predicting fatigue cracking and rutting in full-depth asphalt pavements by centrifuge modeling. To accomplish this task, a small-scale model of a pavement section was constructed. This model was subjected to repeated loading tests in a centrifuge. The model was then removed from the centrifuge to directly measure the resilient tensile strains at the bottom of the asphalt layer and the accumulated permanent deformations near the pavement surface. The centrifuge ensured that the stresses and strains due to self-weight were the same in the small-scale model as in the prototype pavement. Tensile strain was measured instead of observing the fatigue cracking directly because of the very long testing time required for fatigue cracking to occur. The models were tested to 10,000 repetitions, but more than one million repetitions may be required to induce fatigue cracking. A static load test also was performed after the repeated load test.

Model pavements in two different scales (1:10 and 1:20) were constructed, using two different asphalt contents and compaction levels. It was found that the resilient deformations and strains measured in the 1:10 models corresponded well with those in the 1:20 models for all test combinations. Although the permanent deformations displayed a large range of variations, the average of the 1:10 models also correlated with that of the 1:20 models.

Comparisons were made between the model responses and computer solutions. The results of both static and repeated load tests indicate that the deformations and strains of the centrifuge models are greater than those of the computer models. Factors other than the difference in contact conditions may contribute to this discrepancy. For example, the computer models assume that each layer is homogeneous with the same elastic modulus throughout the layer, although the modulus of the sand layer should decrease with the increasing lateral distances from the load. The resilient modulus of the asphalt layer for the computer models was obtained from tests on cylindrical specimens under a stress of 20 psi (138 kPa), which is small compared to an actual loading of 80 psi (552 kPa). If larger stresses were used in the tests, the resilient modulus of the asphalt layer would decrease, and a better match between the centrifuge and computer models could be obtained.

Executive Summary

A knowledge of pavement distress is required to predict the pavement performance of a design. Fatigue cracking and permanent deformation are two types of asphalt pavement distress. Fatigue cracking is caused by tensile strain at the bottom of the asphalt layer. Rutting is caused by accumulated permanent deformations on the road surface. Both permanent deformation and tensile strain are due to the repeated application of wheel characteristics of the materials in the individual layer and the complicated interactions among all layers in the pavement structure.

This study investigated the feasibility of predicting fatigue cracking and rutting in full-depth asphalt pavements by centrifuge modeling. This was accomplished by constructing a small-scale centrifuge model and directly measuring the resilient tensile strains at the bottom of the asphalt layer and the accumulated permanent deformations on the pavement surface under repeated loads. The purpose of using a centrifuge is to ensure that the stresses and strains due to self-weight are the same in the small-scale model as in the prototype pavement. The reason for measuring the tensile strain rather than observing directly the fatigue strain was due to the very long testing time required for fatigue cracking to occur. The models were tested to 10,000 repetitions, but more than one million repetitions may be required to induce fatigue cracking. A static load test was also performed after the repeated load test.

Model pavements in two different scales (1:10 and 2:20) were constructed, using two different asphalt contents and compaction levels. It was found that the resilient deformations and strains measured in the 1:10 models corresponded well with those in the 1:20 models for all test combinations. Although the permanent deformations displayed a large range of variations, the average of the 1:10 models also correlated well with that of the 1:20 models.

Comparisons were made between models responses and computer solutions. The results of both static and repeated load tests indicate that the deformations and strains obtained by the centrifuge models are greater than those by the computer models. Other than the difference in contact conditions as previously explained, other factors may also contribute to this discrepancy. For example, the computer models assume that each

layer is homogeneous with the same elastic modulus throughout the layer, whereas the modulus of sand layer should decrease with increasing lateral distances from the load. The resilient modulus of asphalt layer for the computer models was obtained from tests on cylindrical specimens under a stress of 20 psi (138 kPa), which is small compared to an actual loading of 80 psi (552 KPa). If larger stresses were used in the tests, the resilient modulus of asphalt layer would decrease and a better match between the centrifuge and computer models could be obtained.

The effect of the centrifuge on model responses was investigated by conducting 1g tests in which the same repeated load was applied to 1:20 models by dead weights without the 20g centrifugal force. It was found that the average resilient deformations of 1g tests were five times greater than those of 20g tests, and the resilient strains and permanent deformations were also two to four times larger. The large influence of the centrifuge is not due to the effect of self-weight, but rather is due to the lack of contact between the prefabricated asphalt layer and the subgrade. This conclusion is supported by the fact that both the resilient strains and deformations obtained by the 1:10 models are slightly greater than those by the 1:20 models. Strains and deformations obtained from both model tests are greater than those by the computer models based on full contact.

The testing of small-scale models requires the use of small aggregates for the asphalt mix. To be sure that the deformation characteristics of coarse asphalt mixes can be reproduced by this fine-aggregate mix, cylindrical asphalt specimens of fine, medium, coarse, and very coarse mixes were fabricated and their properties were compared. It was found that the deformation characteristics of the coarser mixes, when designed by the Marshall procedure, did not vary significantly, and fell within the range of the fine mix simply by varying the asphalt content and density of the fine mix.

Chapter 1 Introduction

1.1 Scope of Investigation

This report summarizes the results of a preliminary study on the feasibility of using small-scale centrifuge models for predicting the fatigue cracking and rutting in asphalt pavements. Although the technique of centrifuge testing is not new and has been used frequently in geotechnical engineering (Cheney, 1982), the concept has not been applied to pavement research anywhere in the world. This study was supported by the Strategic Highway Research Program as an IDEA (Innovation Deserving Exploratory Analysis) project.

The basic idea of centrifuge testing is to construct a small-scale pavement model similar to the prototype pavement structure and subject it to centrifugal forces, so that the stresses and strains due to self weight are the same as those in the prototype pavement. This model is then subjected to repeated loads with the same stress levels as in the prototype pavement. The horizontal resilient tensile strain at the bottom of asphalt layer and the accumulated permanent deformations on the pavement surface under increasing load repetitions can be measured directly. The reason for measuring the resilient tensile strain rather than observing the fatigue cracking directly is due to the very long testing time required for fatigue cracking to occur. The models were tested to 10,000 repetitions but more than one million repetitions may be needed to induce fatigue cracking.

One method to check the validity of centrifuge testing is by applying the "modeling of models" concept. This concept implies that a small-scale model can be modeled by an even smaller model. The 1:20 model can be used to model the 1:10 model. All the deformations in the 1:20 model should be one half of

those in the 1:10 model but the dimensionless tensile strains should be the same. In other words, no matter what scale factors are used, the same results should be obtained when scaled back to the prototype. The major scope of this study was to check the "modeling of models" concept and compare the experimental measurements with the theoretical solutions obtained by the VESYS and KENLAYER computer programs.

This report is a condensed version of a doctoral dissertation by Roghani (1990). Many of the additional tests and analysis reported in the dissertation will not be presented here because of inconclusive results based on limited data. However, these additional tests and analysis do support the conclusions that the "modeling of models" concept is valid and that the results of centrifuge testing compare reasonably with the computer solutions. Readers interested in these additional tests and the details of instrumentation and testing procedures should refer to the dissertation by Roghani (1990).

1.2 Nature of Problem

To predict the pavement performance as a basis for design, a knowledge of pavement distress is required. Two types of distress in asphalt pavements are the fatigue cracking and permanent deformation. The fatigue cracking is caused by the tensile strain at the bottom of asphalt layer and the rutting is caused by the accumulated permanent deformations on the road surface, both due to the repeated applications of wheel loads. The prediction of fatigue life and rut depth in asphalt pavements is a complex problem. This complexity is indicated by the numerous comprehensive investigations on the characteristics of paving materials and the performance of pavement structures. The pavement performance under service conditions is affected by both the characteristics of the materials in the individual layer and the complicated interactions among all layers in the pavement structure.

The current method of predicting fatigue cracking and rutting is to test the paving materials, such as hot mix asphalt, untreated granular materials,

and subgrade soils, separately in an arbitrary manner and input their properties into a computer model, such as the various versions of VESYS structural system (Kenis et al., 1982). However, due to the large number of factors involved, it is difficult to verify the validity of the method. The outcome of prediction may change significantly depending on the arbitrary input data derived from test conditions different from those in the pavement systems. The use of centrifuge models makes possible the testing of all paving materials as a unit with the same loading and boundary conditions as in the prototype pavement. Instead of evaluating the fatigue properties of hot mix asphalt by conventional beam or indirect tensile tests and the deformation characteristics of cylindrical specimens under arbitrary boundary and loading conditions, the parameters affecting the fatigue cracking and permanent deformation are measured directly in the centrifuge model, taking into account the interactions among all layers.

One disadvantage of small-scale models is the necessity of using small aggregates for the asphalt mix and the granular base. It is generally agreed that, under extremely heavy wheel loads, the use of extra large aggregates can reduce the rut depth. However, the replacement of large aggregates by small aggregates should not be a cause for concern under normal conditions because the factors affecting the resilient and permanent deformations of asphalt mixes are the same as those affecting the fatigue cracking and are practically independent of the size of aggregates. These factors include the stiffness modulus of asphalt and the volume of asphalt and aggregate as a percentage of the total volume (Shell, 1978). A comparison of the deformation characteristics of fine asphalt mixes with those of medium, coarse and very coarse mixes, as obtained from this study, clearly indicates that, when designed by the Marshall method, the resilient modulus, creep compliance, and permanent deformation parameters of these coarser mixes do not vary significantly and fall within the range of the fine mix by simply varying the asphalt content and density of the fine mix.

The complexity of the factors that govern the response of flexible pavement systems usually deters the use of theoretical methods to predict the

pavement behavior. Consequently, verification of pavement design is required to insure that the pavement will function as expected. It is well known that the construction of full scale asphalt pavements for testing is the most valid method of verification. However, this method is not only time consuming but is also very expensive. The use of centrifuge tests to verify the design assumptions is much cheaper and quicker and can be easily controlled in the laboratory. It should be noted that the centrifuge test can only verify the theory as used in design and is not a substitute for field tests. The results of centrifuge tests are valid only under the testing conditions in the laboratory and their extensions to actual field conditions need further correlations.

1.3 Objectives of Research

The purpose of this study was to investigate the possibility of predicting the fatigue cracking and rutting of a full depth asphalt pavement by centrifuge modeling. This was achieved by constructing small-scale models composed of a fine asphalt mix on a sand subgrade and testing them in the centrifuge under repeated loading. The resilient tensile strains at the bottom of asphalt layer and the accumulated permanent deformations on the surface of the pavement were measured directly as the number of load repetitions increased. Because the test was relatively nondestructive, a static load test also was performed after the repeated load test when the model had been fully recovered. More specifically the objectives of the research were:

1. To design the instrumentation for centrifuge testing, including the fabrication of capsule and loading mechanism and the setup of data acquisition system for an IBM personal computer.

2. To determine the resilient and permanent deformation properties of asphalt mixtures containing fine, medium, coarse and very coarse aggregates and check whether the properties of the coarser mixes can be simulated by the fine mix.

3. To develop procedures for fabricating small-scale models in two different scale factors of 1:10 and 1:20, each consisting of two different asphalt contents of 8.7 and 7.0% and static compaction levels of 200 and 300 kip (0.89 and 1.34 MN), and check the "modeling of models" concept.

4. To find the effect of centrifuge on model responses by applying the same load to the 1:20 model, one with the centrifuge and the other without the centrifuge.

5. To model a prototype pavement and compare the strains and deformations obtained from the model tests with those predicted by the VESYS computer model developed by the Federal Highway Administration (FHWA, 1976) as well as by the KENLAYER program developed at the University of Kentucky (Huang, 1990).

Chapter 2 Centrifuge Facility and Instrumentation

2.1 Basic Concept

Figure 2.1 is a schematic diagram showing the components of pavement and loading for both the prototype and the small-scale models. The pavement is composed of a layer of sand asphalt (fine mix) with a thickness of h_1 and a sand subgrade with a thickness of h_2 and is underlain by a rigid base. Loads are applied to the pavement through a circular disk with a diameter of D. The small-scale pavement can also be considered as infinite in areal extent because the distance from the load to the circumferential boundary is very

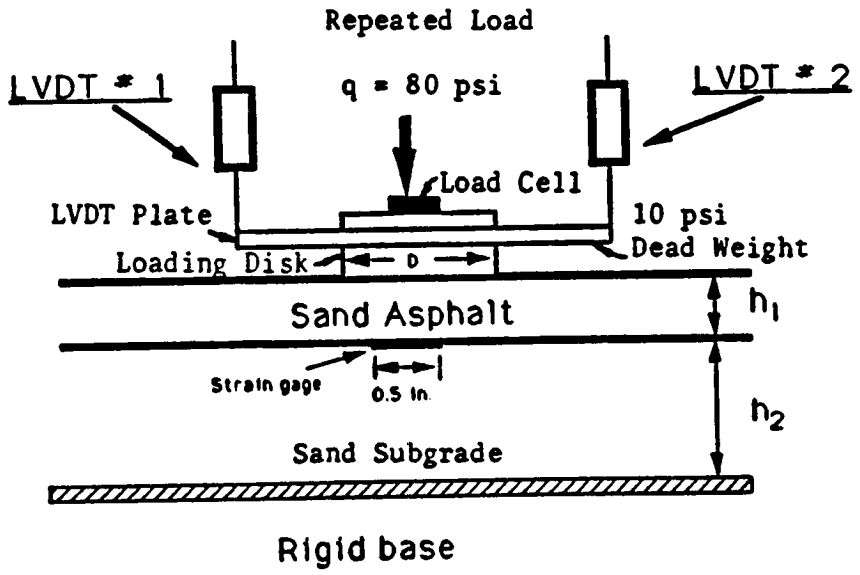

Figure 2.1 Schematic diagram of prototype pavement and small-scale models (1 in. = 25.4 mm, 1 psi = 6.9 kPa)

large compared to the radius of the loaded area (Huang, 1969). The loading consists of a repeated load of 80 psi (552 kPa) and a static load of 10 psi (69 kPa). The application of a static load prior to the repeated load does not simulate the actual prototype pavement insitu but is necessary due to the weight of LVDT (Linear Variable Differential Transformer) plate under the centrifugal forces.

Pavement Response

Based on the Burmister's layered theory (Yoder and Witczak, 1975), the deformation, stress and strain at any point in a layered system can be expresses as

$$s = q\, F_s \tag{2.1}$$

$$w = \frac{q\, D\, F_w}{E_s} \tag{2.2}$$

in which s = stress or strain, q = average contact pressure, or the total load divided by the contact area, F_s = stress or strain factor, w = deformation, D = diameter of loaded area, E_s = modulus of subgrade, and F_w = deformation factor. Note that F_s and F_w depend on the dimensionless ratios, h_1/D and h_2/D, as well as the properties of the material in each layer. As long as the contact pressure, q, and the ratios, h_1/D and h_2/D, are the same, the stress and strain will be the same but the deformation will be proportional to the diameter of the loaded area, D. In other words, a small-scale model with a smaller loaded area can be used to simulate a prototype pavement with a larger loaded area if the other linear dimensions are reduced proportionally.

Although the small-scale model can reproduce the same stresses and strains in a prototype pavement under an externally applied load, the stresses and strains in a small-scale model due to the self weight are much smaller than those in a prototype pavement. Therefore, it is necessary to place the

small-scale model in a centrifuge capsule and rotate at such a speed that the same self weight is obtained.

Centrifugal Force

In centrifuge testing, the centrifugal force is assumed to be concentrated at the centroid of the specimen and expressed in terms of g, which is the acceleration due to gravity. When the capsule rotates at a constant speed, the centrifugal force can be written as

$$F = \frac{m\ V^2}{R} \tag{2.3}$$

in which F = centrifugal force, m = mass, V = tangential velocity, and R = radius of rotation. Eq. 2.3 is based on the assumption that the centrifugal force is horizontal and the weight due to the normal gravity is neglected. This approximation should involve very little error because the centrifugal force is 10 to 20 times greater than the normal gravity. The centrifugal force can also be written in terms of normal gravity by

$$F = m\ N\ g \tag{2.4}$$

in which N = multiple of gavitational acceleration. From Eq. 2.3 and 2.4

$$N = \frac{V^2}{gR} \tag{2.5}$$

When R is in ft, T is the angular velocity in rpm, and g is 32.2 ft/sec^2 (9.81 m/sec^2), or 115,920 ft/min^2 (35,340 m/min^2).

$$N = \frac{(2\pi RT)^2}{gR} = \frac{T^2\ R}{2936} \tag{2.6}$$

$$T = \sqrt{\frac{2936\ N}{R}} \qquad (2.7)$$

In view of the fact that the purpose of using centrifuge is to simulate actual self weight, the distance from the top of subgrade to the center of rotation, or R = 3.83 ft (1.17 m), was used in Eq. 2.7 to determine the rpm required.

Scale Factors

To verify the "modeling of models" concept, two different scale factors were used in this study. Table 2.1 shows the dimensions and weights of the prototype and the small scale models. The prototype pavement to be modeled is composed of 10 in. (254 mm) of asphalt layer over 30 in. (762 mm) of subgrade on top of a rigid base. The load is applied over a rigid plate having a diameter of 12 in. (305 mm). The values tabulated are explained below:

Table 2.1 Prototype versus Small-Scale Centrifuge Models

Type	Prototype	1:10 Model	1:20 Model
Loading Diameter, D (in.)	12	1.2	0.6
Asphalt thickness, h_1 (in.)	10	1.0	0.5
Subgrade Thickness, h_2 (in.)	30	3.0	1.5
Angular Velocity, T (rpm)	0	88	124
Weight of Loading ram (lb)	9050	9.53	1.19
Weight of LVDT plate (lb)	1131	0.88	0.11

Note: 1 in. = 25.4 mm, 1 lb = 4.45 N

1. The dimensions, D, h_1 and h_2, of the 1:10 model are 1/10 of the prototype, while those of the 1:20 model are 1/20 of the prototype.

2. The angular velocity T in rpm is computed from Eq. 2.7 with R = 3.83 ft (1.17 m), which is the distance from the center of rotation to the top of subgrade. For the 1:10 model, with N = 10, $T = \sqrt{2936 \times 10/3.83} = 88$ rpm. For the 1:20 model, $T = \sqrt{2936 \times 20/3.83} = 124$ rpm.

3. The weight of loading ram is based on a contact pressure of 80 psi (552 kPa). For the 1:10 model with a loading diameter of 1.2 in. (31 mm), the total load is 90.5 lb (403 N). The distance, R, between the center of gravity of the loading ram and the center of rotation is 3.6 ft (1.1 m) when the ram hits the pavement surface. When the centrifuge is rotated at 88 rpm, the multiple of gravitational acceleration can be computed by Eq. 2.6, or $N = (88)^2 \times 3.6/2936 = 9.5$. Therefore, the weight of loading ram should be 90.5/9.5 = 9.53 lb (42.4 N). For the same contact pressure and radius of rotation, the weight of loading ram for the 1:20 model should be 1.19 lb (5.3 kN), which is one-eighth of that for the 1:10 model. It should be pointed out that the actual load applied to the model was measured by a load cell. The use of these weights is to approximate a contact pressure of 80 psi (552 kPa). If the measured load is different, the measured deformation and strain should be corrected by direct proportion.

4. The weight of LVDT plate multiplied by the multiple of gravitational acceleration plus the force exerted by the LVDT spring should result in a contact pressure about 10 psi (69 kPa).

2.2 Centrifuge

A centrifuge with a capacity of 6,000 g-lb (27 g-kN) was extensively modified to make it capable of testing small-scale models under both repeated and static loading. The facility is located in an isolated section of the Daniel V. Terrell Civil Engineering Research Laboratory. This laboratory houses a complete soil mechanics laboratory, a machine shop and the necessary

instrumentation for the operation and maintenance of the centrifuge. As shown in Figure 2.2, the centrifuge consists of the following basic components:

1. Rotating arm and counterweight.
2. 2-HP electrical motor and gear reduction.
3. Structural frame to support the drive shaft connected to the rotating arm.
4. Protective housing and wall of sand bags.
5. Slip ring assembly to pass the lead wires from the transducers in the test capsule to the signal conditioner.
6. Encoder to measure the angular velocity in rpm.
7. Test capsule to house the small-scale model to which the repeated and static loads are applied.

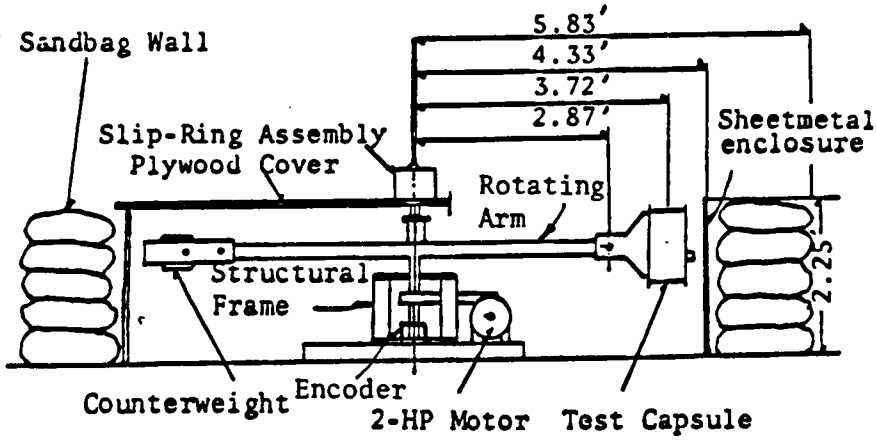

Figure 2.2 Major components of centrifuge
(1 ft = 0.305 m)

2.3 Test Capsule

A view of the test capsule mounted on the centrifuge arm is shown in Figure 2.3. Starting from the bottom, the capsule consists of lower base plate and plexiglass cylinder, pavement model, LVDT plate, capsule lid and loading device, as shown in Figure 2.4 for the 1:10 model.

Lower Base Plate and Plexiglass Cylinder

The base plate and the plexiglass cylinder together serve as the housing for the small-scale model. The plexiglass cylinder has an inside diameter of 11.5 in. (292 mm) and is fitted snugly into a groove on the lower aluminum base plate. The base plate and plexiglass cylinder are connected to the capsule lid by 8 threaded rods. The thickness of base plate was 0.5 in. (13 mm). For the 1:10 model, the subgrade was placed directly on the base plate. For the 1:20 model, three aluminum plates, each 0.5 in. (13 mm) thick, were placed above the base plate to reduce the thickness of the subgrade.

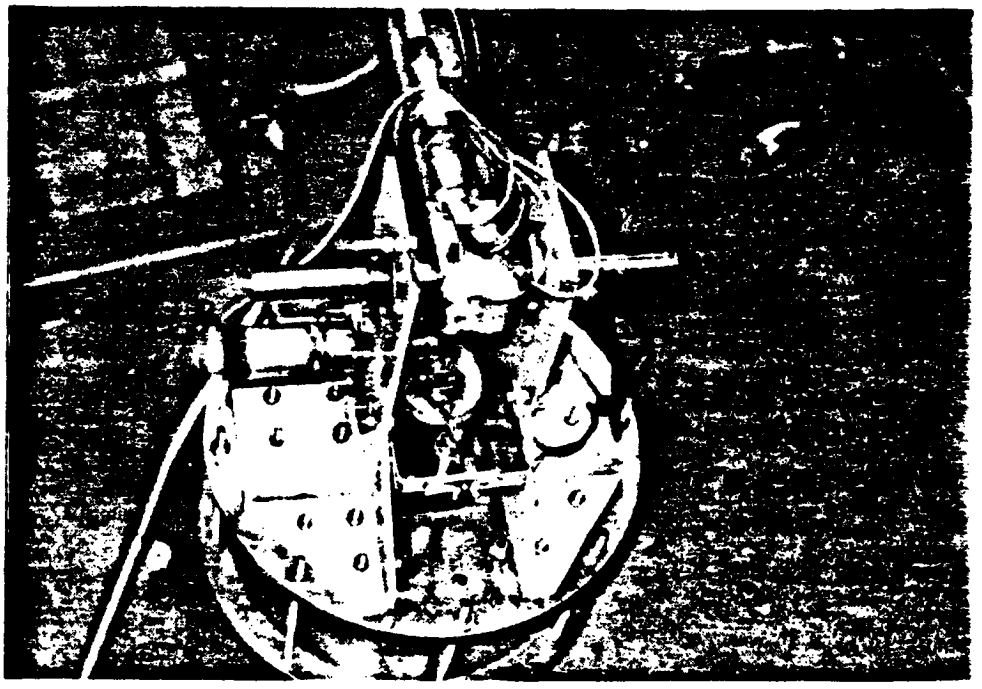

Figure 2.3 A view of centrifuge test capsule

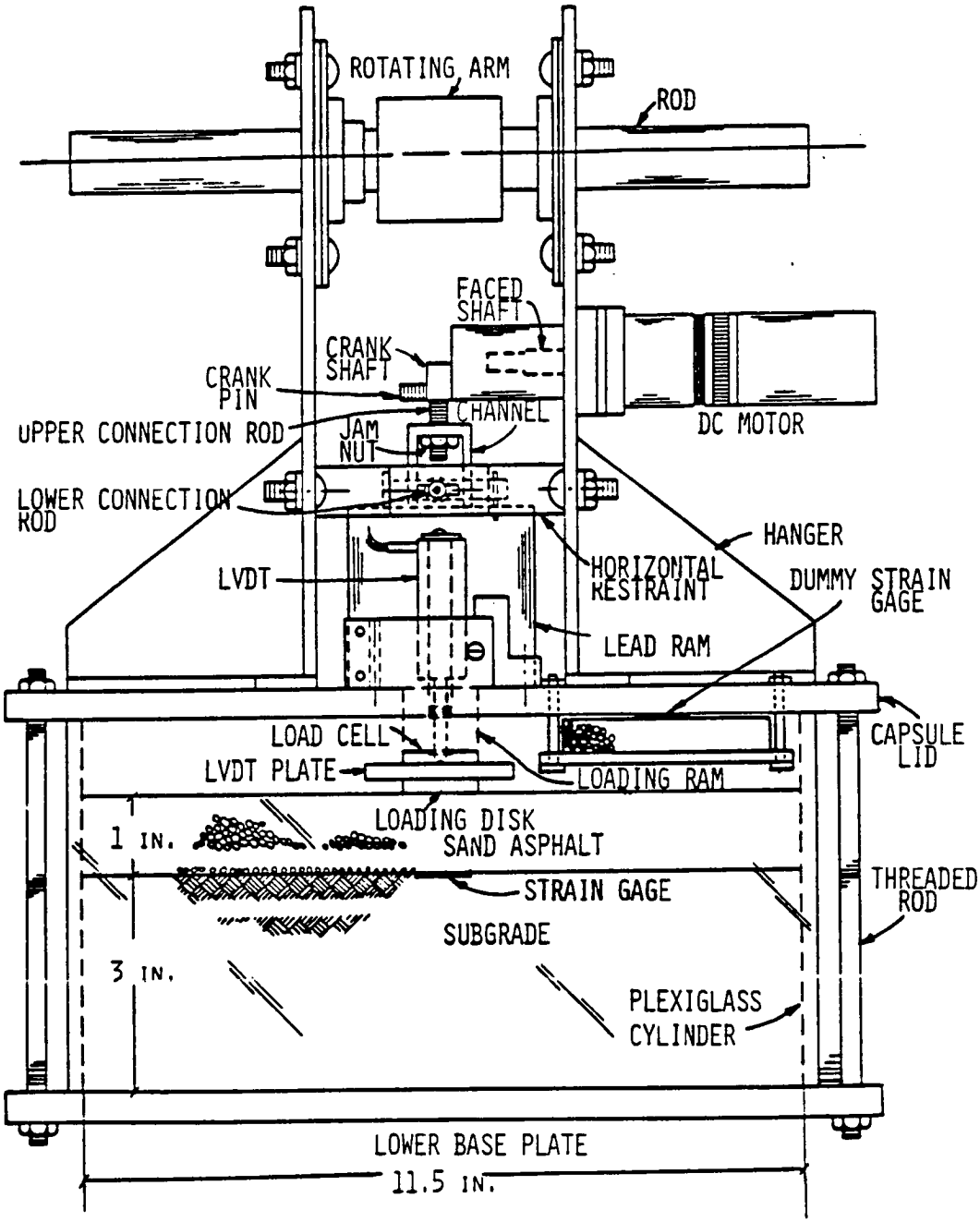

Figure 2.4 Schematic diagram of centrifuge capsule
(1 in. = 25.4 mm)

Pavement Model

The pavement model consisted of a sand subgrade overlain by a sand asphalt layer. The strain on the bottom of the asphalt layer was measured by a strain gage glued to the lower surface of the asphalt directly below the center of the loaded area. As the asphalt specimen is strained due to induced loads, changes in electrical resistance of the strain gages occur. A dummy strain gage for temperature compensation was mounted on a small block of asphalt specimen and placed on a platform bolted to the bottom of the capsule lid, as shown in Figure 2.4.

LVDT Plate

Two LVDT plates were designed for the two models. Each plate consists of a top circular disk, which holds a miniature load cell with a capacity of 250 lb (1.11 kN), a main plate, and a circular loading disk. All three pieces were bolted together by two flat-head screws. The main plate for the 1:20 model was made of aluminum, while the main plate for the 1:10 model was made of steel. The top disk, to which the load cell was attached, was used for both models.

Capsule Lid and Hanger

An aluminum plate is fitted on the top of the cylinder as a lid. A groove was machined on the bottom of the plate for the plexiglass cylinder. Two hangers made of steel plate are bolted to the top of the lid to act as mounting brackets which allow the testing capsule to be attached to the centrifuge rotating arm. The deformation at the surface of the pavement model due to the applied load was measured by two LVDTs located diametrically opposite each other at a radial distance of 2.1 in. (53 mm) from the center. The LVDTs were mounted on the lid and passed through the holes on the lid with the lower end in contact with the LVDT plate.

Loading Device

A special loading device was designed and constructed to apply the repeated load to the model. The loading mechanism consists of D.C. electrical motor, faced shaft, crank shaft, crank pin, upper and lower connection rod, channel, jam nut, lead ram, and loading ram, as shown in Figure 2.4. The speed of the motor is controlled by a variable power supply. The loading and rest periods can be adjusted by turning the jam nut up or down. Figure 2.5 shows the different loading waveforms which can be generated. The 0.1 sec loading and 0.9 sec rest waveform has been used most widely to simulate the traffic. However, in this research the 0.45 sec loading and 0.55 sec rest waveform was used because it gave more consistent results. A mechanism was designed for providing horizontal restraint to the loading ram so that a vertical loading with no eccentricity could be applied.

Loading Frame for 1g Test

A special loading frame was designed and constructed for the purpose of applying the 80 psi (552 kPa) repeated load to the 1:20 model without centrifugal forces. Since no centrifugal forces are applied, this test is

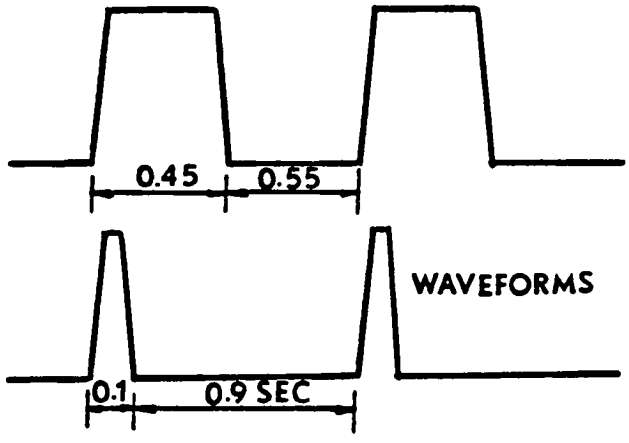

Figure 2.5 Different waveforms of repeated load

referred to as the 1g test. The loading mechanism consists of a frame, a base plate and the dead weight. The base plate fits on the top of the loading ram through a hole in the middle of the plate. The frame is bolted to the end of the base plate by two allen screw bolts. The known dead weight is placed on the top of the frame and fastened in place by fiber tapes. Figure 2.6 shows the loading frame and the dead weight for the 1g test. The test was conducted by placing the capsule on the ground near to the rotating arm. The small motor raised the loading ram together with the loading frame and applied the required load on the pavement model.

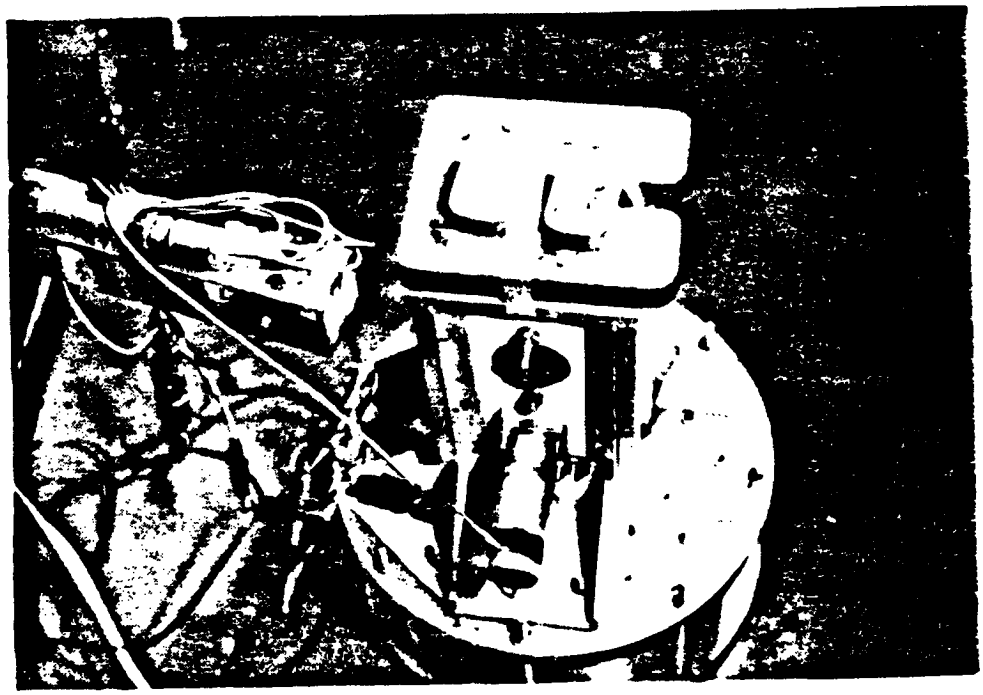

Figure 2.6 Loading frame with dead weight for 1g test

2.4 Data Aquisition Systems

An IBM PC was used together with Labmaster data acquisition boards to perform the required data acquisition and reduction. Figure 2.7 shows schematically how different parts of centrifuge apparatus are interconnected. The DC signal output from the LVDTs, load cell and strain gages was routed through the Sensotec signal conditioner to the Labmaster boards, while the encoder was routed via a frequency/voltage converter.

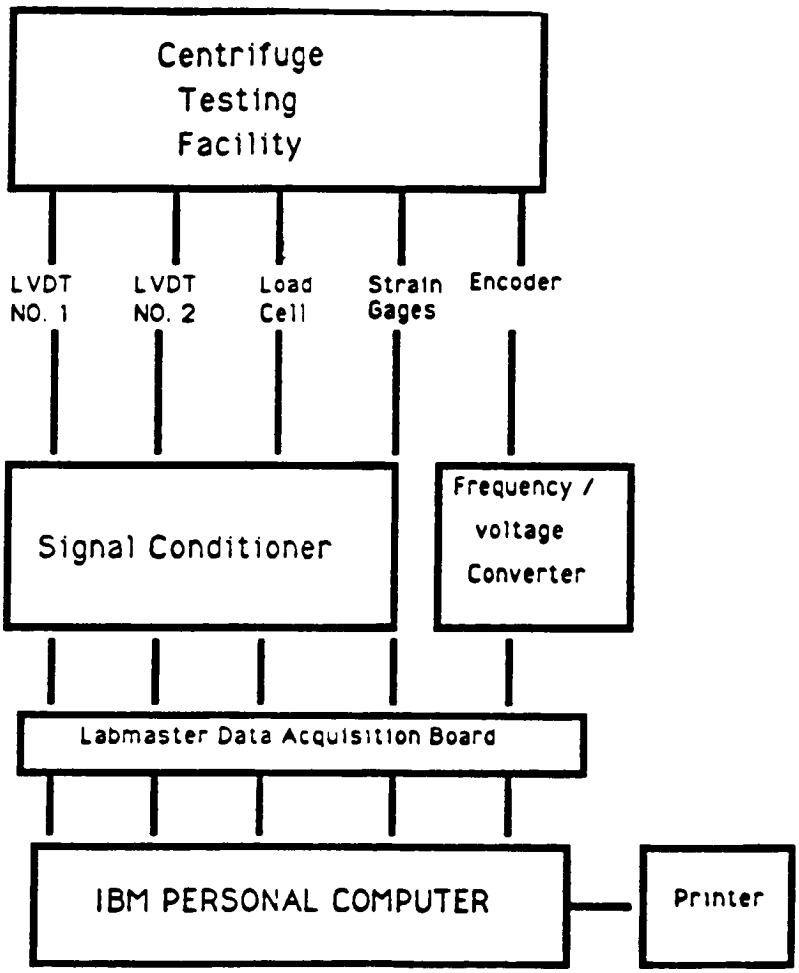

Figure 2.7 Data aquisition system for centrifuge facility

Labmaster Boards

Labmaster is a multi-function high-speed analog/digital laboratory analysis tool. It is constructed out of two printed circuit boards, one called the mother board and the other called the daughter board. The mother board contains the digital logic and plugs directly into the IBM PC bus. The daughter board contains all the analog acquisition circuitry. The data acquisition board converts the continuous analog signal into a 12 bit digital signal that the computer can use and store.

Labtech Notebook

The Labtech Notebook is a commercially available software package for data acquisition, monitoring, process control, and analysis which runs on an IBM PC. The software is a menu driven program. Each data acquisition run may be set up differently, depending on the type of test. Each channel may have different setup conditions, such as scale factor, sample rate, stage, duration, etc. When the data acquisition is operated at a normal speed mode, the data is streamed continuously to the hard disk installed on the IBM PC. At the normal speed mode, the real time display function is available and the digital panel meter indicates the transducer outputs for different channels at real time, which can be used to monitor the test result at different steps of the test.

The data files from Labtech Notebook are stored in an ASCII format. Labtech Notebook has been designed to interface with Lotus 123 for additional functions. As a result, the data from the tests can be imported directly into a Lotus 123 spread sheet program for further analysis and plotting.

Lotus 123

The Lotus program was used to create input data file from the raw data to be used by the ANALYZER program. Lotus was used for initial inspection of

repeated load data by graphing the output versus time for possible involvement of noise in the data. The raw data from the sequential data files created by Labtech Notebook were imported into Lotus. The load, average LVDT output and strain for repeated load testing were measured at time sequences of 0-15, 195-205, 995-1005, 3995-4005, and 9995-10005 sec at a sampling frequency of 20 Hz. Because the load was applied at a rate of one repetition per second, the time in seconds was equivalent to the number of load repetitions. The same time sequences were used for the static load except that the test was stopped at 1005 sec.

Analyzer

An ANALYZER program was developed to analyze data from repeated load tests. The program was interactive and user friendly. It was designed to perform median filtering and average processing of the data, to print graphs of load, LVDT output and strain after average processing at different time sequences, and to create files containing the averaged deviator load, resilient and permanent deformations, and resilient and permanent strains at different time sequences.

Chapter 3 Materials and Fabrication of Asphalt Specimens

3.1 Materials

The materials used in this study include asphalt mixtures for fabricating the centrifuge and cylindrical specimens and a river sand for constructing the subgrade of small-scale models.

Asphalt Mixtures

The asphalt mixture used for the small-scale model is a fine mix containing asphalt contents of 8.7% and 7%. To compare the properties of the fine mix with those containing larger aggregates, cylindrical specimens containing fine, medium, coarse and very coarse aggregates were fabricated. The asphalt cement used for all mixes was an AC-20 obtained from the Ashland Oil Company, Ashland, Kentucky. The properties of the asphalt are listed in Table 3.1.

Table 3.1 Properties of Asphalt Cement

Penetration at 77 F, 100g, 5 sec	80
Viscosity at 140 F (poise)	1817
Viscosity at 275 F (poise)	412
Viscosity of residual after thin film oven test at 140 F (poise)	3816
Penetration of residual % of original (%)	48
Ring and ball softening point (°F)	120
Specific gravity	1.02

The aggregates used for all mixes were obtained by blending various sizes of limestone and a limestone sand. The gradation and specific gravity of aggregates for the various mixes are shown in Table 3.2. The gradation of fine mix conforms to the sand asphalt surface, Type I, as specified by the Kentucky Department of Transportation. The coarse and very coarse mixes have the same gradation for particles smaller than 3/4 in. (19 mm) but any particles larger than 1 in. (25 mm) in the very coarse mix were replaced by the same weight of materials between 3/4 in. (19 mm) and 1 in. (25 mm) in the coarse mix.

Table 3.2 Gradation and Specific Gravity of Aggregates for Various Mixes

Sieve Size	Fine	Medium	Coarse	Very Coarse
2 in.	--	--	--	100
1.5 in.	--	--	--	99
1 in.	--	--	100	77
3/4 in.	--	--	65	65
1/2 in.	--	--	54	54
3/8 in.	--	100	44	44
No. 4	--	88	29	29
No. 8	100	79	23	23
No. 16	90	63	15	15
No. 30	75	48	9	9
No. 50	45	33	5	5
No. 100	15	21	2	2
No. 200	6	10	1	1
Bulk S. G.	2.61	2.61	2.56	2.56
Apparent S. G.	2.71	2.71	2.71	2.71

Note: 1 in. = 25.4 mm

The results of Marshall tests for the four mixes are presented in Table 3.3. Due to the large aggregate size used in the coarse and very coarse mixtures, the Marshall specimens were compacted in a mold 6 in. (152 mm) in diameter and 3.75 in. (95 mm) in height by a 22.5 lb (100N) Marshall hammer.

Table 3.3 Summary of Marshall Test Results

Type of Mixture	Maximum Stability (lb)	Maximum Unit Weight (pcf)	Optimum Asphalt Content (%)
Fine	1965	140.2	8.7
Medium	1960	148.1	7.2
Coarse	4100	147.4	4.3
Very Coarse	5000	147.3	4.7

Note: 1 lb = 4.45 N, 1 pcf = 157.1 N/m^3

SAND

The sand used for the subgrade in the small-scale pavement models was a uniformly graded, dry Boonesboro river sand. Figure 3.1 shows the gradation of the sand. The sand had an angle of internal friction of 37°, which corresponds to a coefficient of earth pressure at rest, K_o, of 0.4.

3.2 Centrifuge Specimens

The centrifuge asphalt specimens were 11.5 in. (292 mm) in diameter and approximately 1 in. (25 mm) thick for the 1:10 model and 0.5 in. (13 mm) thick for the 1:20 model. Due to the thin specimens used, only the fine mixture was used to fabricate the centrifuge specimens.

Equipment

A mold and a rigid disk were constructed for the fabrication and

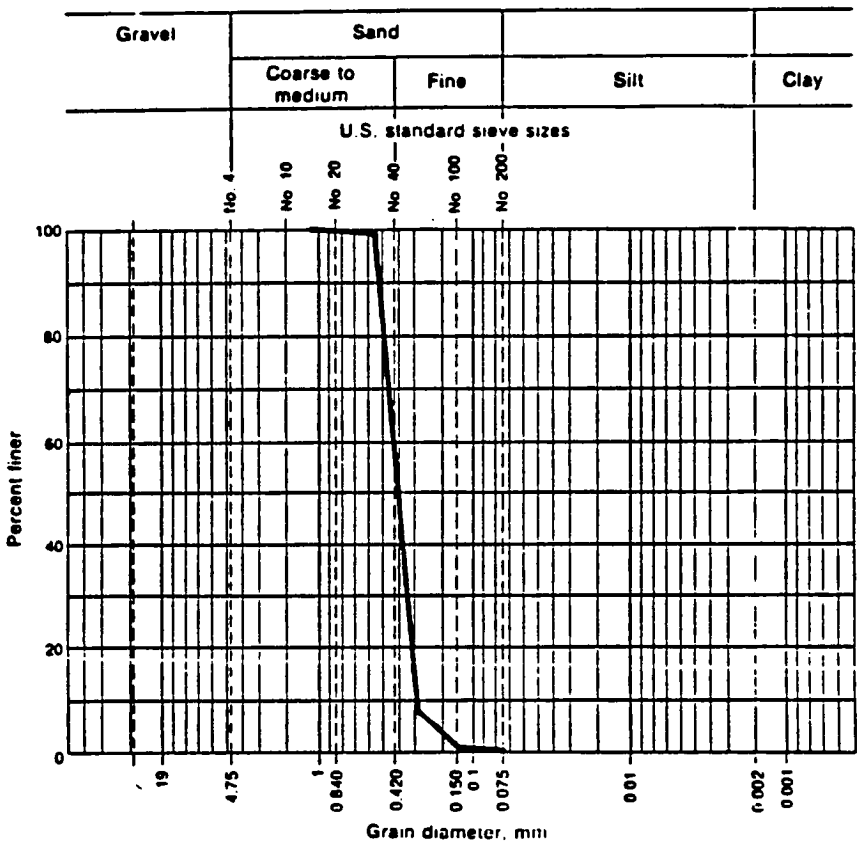

Figure 3.1 Grain size curve of sand

compaction of centrifuge specimens. The mold has an inside diameter of 11.5 in. (292 mm) and a height of 4 in. (102 mm) The wall is composed of two curved steel plates screwed at the bottom to a 0.5 in. (13 mm) steel plate. The rigid disk is made of two cylindrical aluminum pieces bolted together. The bottom piece has a diameter of 11.5 in. (292 mm) and a height of 1.5 in. (38 mm) The top piece has a diameter of 6 in. (152 mm) and a height of 4 in. (102 mm) A universal compression testing machine with a capacity of 300 kips (1.33 MN) was used for fabricating all the asphalt specimens.

Mix Composition

To investigate the validity of centrifuge testing on different mix compositions, the fine mixtures were fabricated with two different asphalt contents: one with an optimum asphalt content of 8.7% and the other with 7%. The specimens were compacted by two different static loads of 200 and 300 kip (0.89 and 1.33 MN). Table 3.4 shows the density and thickness of asphalt specimens with different asphalt contents and compaction levels. Note that specimen No. O8.200 indicates one inch thick asphalt specimen with an asphalt content of 8.7% and a compaction level of 200 kip (890 kN), while H7.300 indicates half inch thick specimen with an asphalt content of 7% and a compaction level of 300 kip (1.33 MN). The thickness of one inch or half inch is the targeted thickness, and the actual thickness is shown in Table 3.4. It can be seen from the table that the densities of specimens compacted by the 200 kip (890 kN) load do not differ significantly from those compacted by the 300 kip (1.33 MN) load.

Table 3.4 Density and Thickness of Centrifuge Asphalt Specimens

Specimen No.	O8.200	O8.300	H8.200	H8.300	O7.200	O7.300	H7.200	H7.300
Density (pcf)	144.0	143.4	144.3	145.6	139.3	142.2	139.7	139.3
Thickness(in.)	1.008	0.990	0.531	0.481	1.036	1.006	0.533	0.513

Note: 1 pcf = 157.1 N/m^3, 1 in. = 25.4 mm

Procedures

The flow chart in Figure 3.2 shows the different steps for fabricating centrifuge specimens. The procedures can be summarized as follows:

1. Approximately 4,000 g of fine aggregate with the gradation shown in Table 3.2 was thoroughly mixed and placed in a pan.

2. The aggregate, mold, compactor, beater, etc. were heated to a temperature of 325°F (162°C).

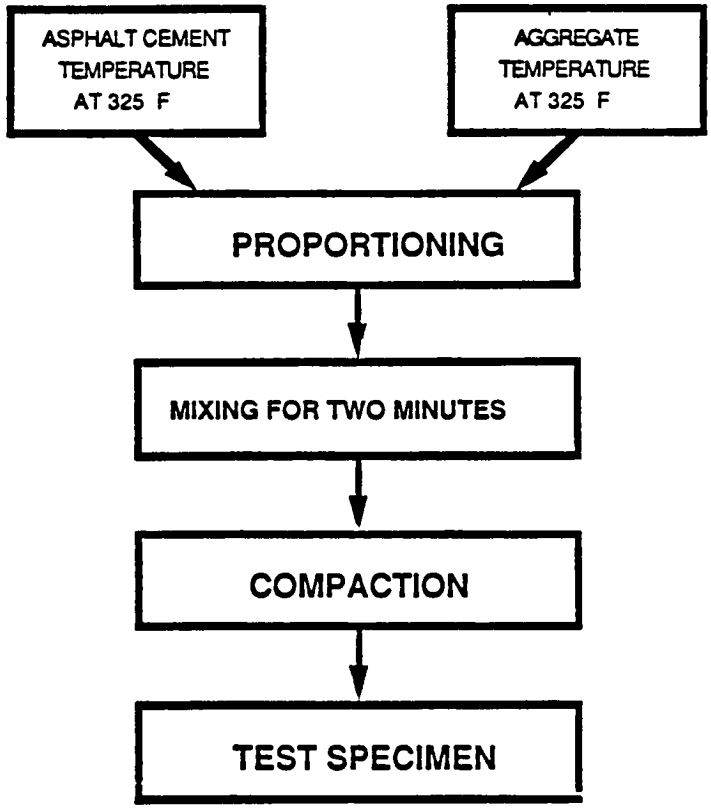

Figure 3.2 Flow chart for fabrication of asphalt specimens

3. Approximately 500 g of AC-20 were heated in a covered can for two hours to 325°F (162°C). This temperature is recommended by The Asphalt Institute (1979) to give viscosities between 150 and 310 centistokes.

4. The heated aggregate was placed in a mixing bowl and weighed by a balance. The required amount of asphalt for the mixture was added to the aggregate in the mixing bowl.

5. The aggregate and the asphalt cement were mixed first with a hot spoon. The mixture was further mixed with a mechanical mixer using a beater for 60 seconds. The side of the bowl was scraped clean with the hot spoon. The mixing was continued for 60 more seconds.

6. The amount of asphalt mixture based on the estimated density for the known volume of compacted specimen was weighed.

7. The weighed mixture was placed in the mold in two layers for the 1:10

model and one layer for the 1:20 model. Each layer was leveled and spaded with a heated rod for 25 times around the perimeter and 25 times over the interior.

8. The rigid disk was placed on top of the leveled asphalt and a static load of 200 or 300 kip (0.89 and 1.33 MN) was applied for 1 minute. The mold was rotated 90 degrees and the same static load was reapplied for 1 more minute.

9. The disk was removed and the specimen was allowed to cool at room temperature. The two curved plates were unscrewed from the base plate, and the specimen was carefully removed.

3.3 Cylindrical Specimens

All cylindrical asphalt specimens had a diameter of 4 in. (102 mm), a height of 8 in. (203 mm), and were compacted by the double plunger method.

Equipment

A steel cylinder with an inside diameter of 4 in. (102 mm) and a height of 12 in. (305 mm) was used as a mold for fabricating the cylindrical specimens. Two plungers having a diameter about 4 in. (102 mm) and a height of 2 in. (51 mm) were made of aluminum and used to compact the specimens by the double plunger method. The specimen was extracted from the mold by pushing it out through a hole on a plate supported by a cylinder having a diameter of 6 in. (152 mm) The same universal testing machine, as used for compacting the centrifuge specimens, was also used for cylindrical specimens.

Mix Composition

Two different asphalt contents of 8.7 and 7% were used for the fine mixtures. These mixtures are the same as used in the centrifuge specimens but were compacted at different compaction levels, ranging from 5 to 67 kip (22 to 298 kN). As cylindrical specimens are difficult to compact to the exact density, they were compacted to different densities, so that the result at any

given density can be obtained by interpolation.

The medium, coarse and very coarse mixes have asphalt contents of 7.2, 4.3 and 4.7%, respectively. These mixes were all compacted under a static load of 40,000 lb. (178 kN) They were not used to fabricate the centrifuge specimen, but only serve as a comparison to the fine mixes.

Table 3.5 shows the different asphalt mixtures for cylindrical specimens. The specimens for the fine mixes are numbered in the same way as the centrifuge specimens. For example, F8.5 indicates a fine mix with an asphalt content of 8.7% and a compaction level of 5 kip (23 kN). Because the medium, coarse and very coarse mixes have only one asphalt content and one compaction level, they are designated by a single letter of M, C and VC, respectively.

Table 3.5 Information on Cylindrical Asphalt Specimens

Specimen No.	F8.5	F8.40	F8.67	F7.20	F7.40	F7.67	M	C	VC
Asphalt content (%)	8.7	8.7	8.7	7.0	7.0	7.0	7.2	4.3	4.7
Compaction Level (kip)	5	40	67	20	40	67	40	40	40
Density(pcf)	137.5	145.8	146.0	138.9	141.7	143.5	149.0	147.4	145.3

Note: 1 kip = 4.5 kN, 1 pcf = 157.1 N/m

Procedures

The flow chart in Figure 3.2 for centrifuge specimens also applies to cylindrical specimens. The initial preparation from steps 1 through 5 are the same as described previously for centrifuge specimens. The latter steps are as follows:

6. The amount of asphalt mixture was weighed on the basis of the targeted density for the known volume of compacted specimen.

7. The mold with the plunger at the bottom was supported by two temporary bars and placed under the compression machine.

8. The mixture was placed in the mold in three layers, each rodded 15

times around the perimeter and 10 times over the interior by a small heated steel rod.

9. The top plunger was placed on top of the uncompacted specimen and an initial load of 500 lb (2.25 kN) was applied to compress the bottom and top plungers and set the mixture against the side of the mold.

10. The temporary supporting bars were removed and the required load, as indicated in Table 3.5, was applied by the full double plunger action for two minutes.

11. The specimen was cooled for 30 minutes at room temperature and then extracted from the mold.

Chapter 4 Testing and Analysis of Centrifuge Models

4.1 Preparation of Pavement Models

The preparation of small-scale models includes the construction of sand subgrade and the installation of centrifuge asphalt specimen on the top of the subgrade.

Sand Subgrade

To eliminate the effect of moisture variation, a dry sand was used for the subgrade. The following steps were used in preparing the sand subgrade for the 1:10 model:

1. The plexiglass cylinder was inserted into the grooved section of the base aluminum plate. Care should be taken that both the groove section of the base plate and the plexiglass cylinder be free of dirt or sand in order to allow the plexiglass to seat completely into the groove section of the base plate.

2. A trial and error method was used to achieve a density of 105 pcf. (16.5 MN/m^3). The required density was obtained by calculating the total mass since the volume was known. The sand was placed in two layers. The volume for each layer was based on a height of 1.5 in. (38 mm) and a diameter of 11.5 in. (292 mm) The sand was weighed and poured into the plexiglass cylinder.

3. The sand was rodded 50 times by a 3/8 in. (9.5 mm) bar uniformly distributed over the area in order to decrease the voids in the sand.

4. The sand was leveled by a screed as shown in Figure 4.1.

5. The sand was compacted to the above density by shaking for 10 minutes in a sieve shaker at a very low speed.

6. The second layer of sand with a height of 1.5 in. (38 mm) was placed into the test capsule by repeating steps 2 through 5.

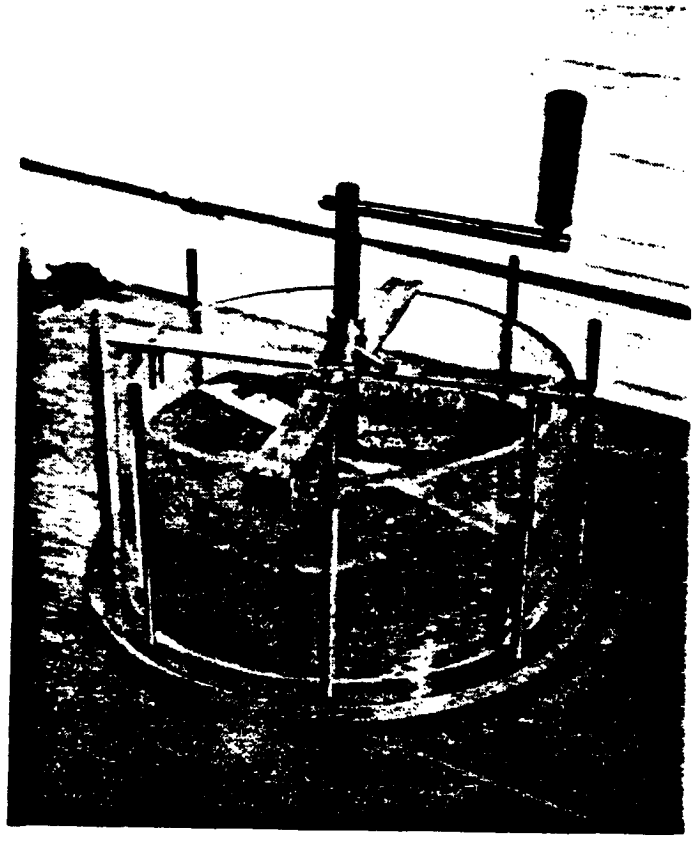

Figure 4.1 Leveling sand in test capsule by a screed

The preparation of the 1:20 model was the same as the 1:10 model except that three aluminum plates, each 0.5 in. (13 mm) in height and 11.5 in. (292 mm) in diameter, were placed on the base plate of the test capsule and that only one layer of sand with a thickness of 1.5 in. (38 mm) was placed on top of the three aluminum plates.

Centrifuge Asphalt Specimen

Procedures for installing the centrifuge asphalt specimen are described

below:

1. The strain gage, after being installed on the asphalt specimen, was checked by a strain gage indicator to make sure that the gage was properly connected.

2. The leads to the strain gage were taped to the asphalt surface by a piece of fiber tape to avoid the straining of the gage.

3. The asphalt specimen was placed on the top of the compacted sand with the strain gage facing down and the lead wires coming out from the side of the specimen.

4. The surrounding area between the side of the specimen and the plexiglass was filled by a caulking material in order to stop the movement of asphalt specimen and the leaking of the sand. Two hours of curing time were needed for the caulking material.

4.2 Installation of Test Capsule

The installation includes LVDT plate, capsule lid with the attached loading mechanism and counterweight.

LVDT Plate

The installation of LVDT plate for the 1:10 model is described below:

1. A double-side tape was cut to a circular shape with a diameter of 1.2 in. (31 mm) and stuck on the bottom of the loading disk of the LVDT plate. The other side of the tape was covered by its protective paper so it did not stick anywhere until step 3.

2. The center of the asphalt specimen, where the load was to be applied, was located. The LVDT plate was placed in such a direction that the two LVDTs were located along the centerline of the plate.

3. After the exact location of LVDT and loading disk was ascertained, the protective cover was removed from the tape and the loading disk was pressed down carefully.

All the steps for the installation of the 1:20 model were the same as

those of the 1:10 model except that a lighter LVDT plate and a loading disk with a diameter of 0.6 in. (15 mm) were used. Figure 4.2 shows the installation of LVDT plate on the pavement surface for the 1:20 model.

Capsule Lid

The installation of the capsule lid is described below:

1. The strain gage and load cell wires were passed through a hole on the lid. Care was taken not to pull the wires during the installation of the capsule lid.

3. The loading ram for the model was inserted through a hole on the lid.

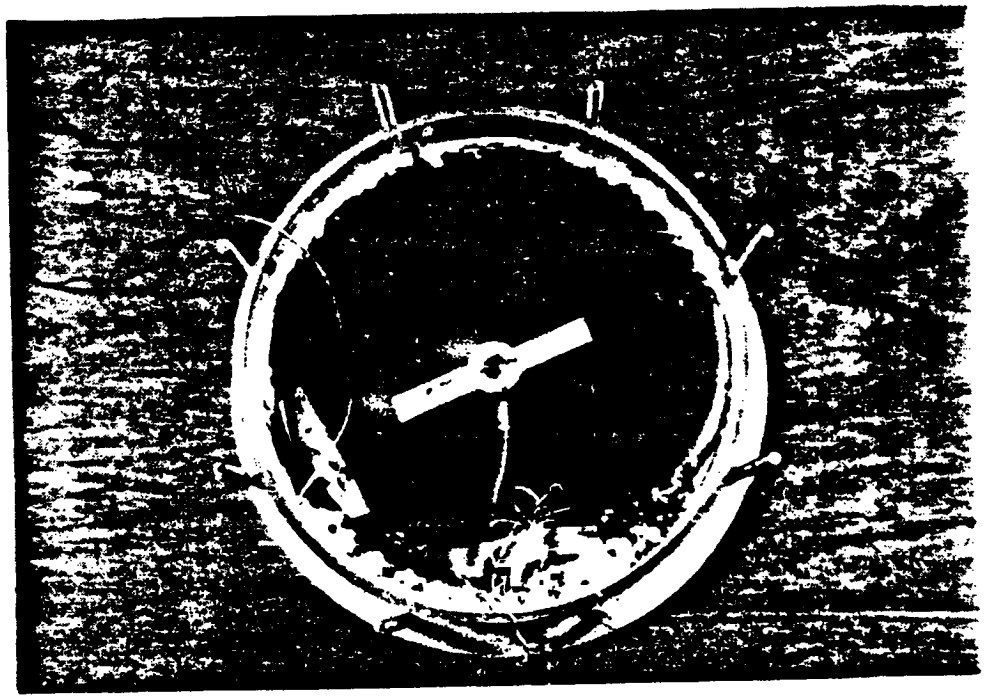

Figure 4.2 A view of LVDT plate on pavement surface for 1:20 model

4. The crank shaft and the loading mechanism was attached to the small motor.

5. The two LVDTs were placed on the LVDT plate through the LVDT mounting blocks and the holes on the lid.

6. The horizontal restraint mechanism was connected to the loading ram so that the load moved vertically up and down without tilting.

Mounting of Capsule and Counterweight

The procedures for mounting the test capsule and the counterweight are described below:

1. The test capsule was weighed and the centrifuge arm was balanced by a counterweight.

2. The counterweight and test capsule on the opposite side of the centrifuge arm were mounted by passing a 1 in. (25 mm) diameter rod through the bearings of the mounting bracket and a hole in the rotating arm.

3. The arm was bolted to the bar by two screws at each end in order to prevent lateral movement of the test capsule and the counterweight.

4. Locking collars were attached to the bearing in order to prevent lateral movement of the test capsule and counterweight while in testing.

5. The waveform for repeated load tests was set by adjusting the jam nut until a loading period of 0.45 sec and a rest period of 0.55 sec were obtained. The waveform was checked by running the repeated load test without centrifuge and graphing the result by Lotus 123.

4.3 Test Procedures

Three types of test were performed. The repeated load centrifuge test was conducted first, followed by the static load centrifuge test. For the 1:20 model, the capsule was removed from the rotating arm and the repeated load 1g test was performed. The different types of test were carried out on the same specimen because the tests were basically nondestructive. It was found that the test results were not affected significantly whether the

specimen had been tested before, as long as a sufficient time was allowed for the specimen to recover.

Repeated Load Centrifuge Tests

For convenience, the repeated load centrifuge test on the 1:10 model is hereafter referred to as the 10g test, while that on the 1:20 model as the 20g test. The procedures described below apply to both 10g and 20g tests:

1. The centrifuge rotation was started by hand in order to decrease the initial load on the drive train.

2. The control switch for the centrifuge motor was turned on and the speed was slowly increased by 5 rpm per minute.

3. The door on the cover of the centrifuge was closed and latched.

4. The speed of centrifuge was increased until 10g or 20g acceleration was achieved, depending on the scale factor.

5. The speed was monitored from the output of the encoder and maintained at the required level for 10 minutes before starting the repeated load test. This was done to improve the contact between the asphalt layer and the subgrade.

6. The monitoring of temperature was started by placing the temperature sensor inside the centrifuge housing.

7. The data acquisition setup program was started.

8. As soon as the program started taking data, the small motor for the loading mechanism was turned on.

9. The electrical timer was started at the beginning of the data acquisition run.

10. The test was run for 10,005 repetitions with data acquired at 1, 10, 100, 1000, 4,000, and, 10,000 repetitions. Except for the first load repetition, the data at each of the above repetitions were the average of 11 repetitions, five above and five below the given repetition.

11. The small motor for the loading mechanism was turned off after 10,005 load repetitions. When the motor was turned off, the load should not be in contact with the specimen.

12. The centrifuge motor was turned off and the rotation slowed to a stop.

Static Load Centrifuge Tests

The static load centrifuge test, also called the 1,000 second creep test, was conducted on both the 1:10 and 1:20 models. All procedures for the static load test were the same as those for the repeated load test except that a different data aquisition program was used and the static load was applied by just turning the motor on until the loading ram hit the surface and then turning it off momentarily.

Repeated Load 1g Tests

The 1g test was performed on the same specimen used for the 20g test. The test was to compare the behavior of the model under the same level of repeated load but without centrifuge. The procedures are described as follows:

1. The test capsule was placed on the floor near the centrifuge arm with all the electrical connections in order.

2. The loading frame was mounted on the loading ram with the dead weights taped on the top of the loading frame. The combined weight of dead load, frame, and loading ram was adjusted to be 22.57 lb (100 N), so a contact pressure of 80 psi (552 kPa) was applied to the model.

3. The remaining procedures are the same as steps 7 to 10, as described for the repeated load centrifuge test.

4.4 Data Reduction

The data obtained from the repeated load tests are the magnitudes of load, the resilient strains at the bottom of asphalt layer, the resilient deformations on the surface, and the permanent deformations on the surface; while those from the static load tests are the magnitudes of load, the strains at the bottom of asphalt layer, and the deformations on the surface. All data for repeated load tests were obtained at 1, 10, 100, 1,000, 4,000 and 10,000

repetitions; while those for static load tests were obtained at 0.05, 0.1, 0.3, 1, 3, 10, 30, 100 and 1,000 sec. Due to the variability of the the applied load and the deformation of the tape and the base plate of the capsule, some corrections on the measured data were made, as will be described below.

Resilient Strains

Because the repeated load applied to the model was not exactly 80 psi (552 kPa) and varied somewhat during the course of the test, a correction of the measured strain was needed. This was accomplished by assuming that the strain was proportional to the load, so the strain under any measured load could be converted to the strain under a load of 80 psi (552 kPa) by direct proportion. Even after this correction, the strains from 100 to 10,000 repetitions still fluctuated slightly. Instead of arbitrarily selecting the strain at a given repetition, say at the 200^{th} repetition as for cylindrical specimens, the average of the resilient strains at 100, 1,000, 4,000 and 10,000 repetitions was used as the resilient strain.

Resilient Deformations

In addition to the correction due to the magnitude of applied load, as described for the resilient strain, two more corrections were made for the resilient deformation. As indicated in Section 4.2, a double-side tape was used to fix the position of the loading disk. The resilient deformation of the tape under a repeated load of 80 psi (552 kPa) was determined using the same setup as the 1g test except that the tape was placed on an aluminum dowel firmly supported on the solid ground, instead of on a pavement model. It was found that the resilient deformation of the tape was 5.28×10^{-4} in. (1.34×10^{-2} mm) Another correction was the resilient deformation of the aluminum base plate under the pavement model. Based on the plate theory and the model calibration (Roghani, 1990), it was found that the resilient deformation of the base plate was 3.27×10^{-4} in. (8.31×10^{-3} mm) for the 10g test and 2.7×10^{-5}

in. ($6.9x10^{-4}$ mm) for the 20g test. Therefore, the total corrections for tape and base plate are $8.55x10^{-4}$in. ($2.17x10^{-2}$ mm) for the 10g test and $5.55x10^{-4}$in. ($1.41x10^{-2}$ mm) for the 20g test. These corrections were deducted from the average resilent deformations measured by the two LVDTs. These corrected deformations were further modified by the magnitude of the applied load. Similar to the resilient strain, the average of the resilient deformations at 100, 1,000, 4,000 and 10,000 repetitions was used as the resilient deformation of the model.

Permanent Deformations

The permanent deformations were measured under both repeated and static loads. The corrections required for permanent deformations take into consideration both the load and the tape. The permanent deformations of the tape were calibrated using the 1g test setup, as described for the resilient deformation. The permanent deformations of the tape under a repeated load of 80 psi (552 kPa) are shown in Table 4.1 and those under a static load of 90 psi (621 kPa) in Table 4.2. The use of 90 psi (621 kPa) for static load is due to the weight of LVDT plate.

Table 4.1 Permanent Deformations of Tape under Repeated Load of 80 psi

No. of Repetitions	1	10	100	1,000	4,000	10,000
Deformation ($in.^{-4}$)	1.27	1.66	2.20	2.89	3.41	3.81

Note: 1 psi = 6.9 kPa, 1 in. = 25.4 mm

After the permanent deformations had been corrected by the tape deformations, they were further modified by the magnitude of the applied load. Because permanent deformations were cumulative, the deformation during each increment, say between 1 and 10 repetitions under the repeated load or 0.05

Table 4.2 Deformations of tape under Static Load of 90 psi

Time (sec)	0.05	0.1	0.3	1	3
Deformation (10^{-4} in.)	0.99	1.07	1.22	1.40	1.59
Time (sec)	10	30	100	1,000	
Deformation (10^{-4} in.)	1.83	2.08	2.39	3.14	

Note: 1 psi = 6.9 kPa, 1 in. = 25.4 mm

and 0.1 sec under the static load, was corrected in proportion to the average load at the beginning and the end of the increment. This corrected deformation was added to the deformation during the first increment, which had also been corrected by the applied load. The corrected deformations for subsequent increments were added to the previous deformation until the last increment was reached.

It is generally assumed that a plot of permanent deformations versus the number of load repetitions on a log-log scale results in a straight line. The measured deformations were analyzed by linear regression to obtain the best fit line, so the permanent deformation at any given repetition could be evaluated.

The deformations under the static load were smoothed out by nonlinear regression between the logarithm of deformations and the logarithm of loading times using a third degree polynomial.

Permanent Deformation Parameters

The method incorporated in the VESYS computer program (FHWA, 1976) for the prediction of rut depth is based on the assumption that the permanent deformation is proportional to the resilient deformation by

$$w_p(N) = \mu\, w\, N^{-\alpha} \tag{4.1}$$

in which $w_p(N)$ = permanent deformation due to a single load application; i.e. at the Nth application; w = resilient deformation; N = number of load applications; μ = a permanent deformation parameter representing the constant of proportionality between permanent and resilient deformations; and α = a permanent deformation parameter indicating the rate of decrease in permanent deformation as the number of load applications increases. The total accumulated permanent deformation can be obtained by integrating Eq. 4.1 with respect to N, or

$$w_p = \int_0^N w_p(N)\, dN = \mu\, w\, \frac{N^{1-\alpha}}{1-\alpha} \tag{4.2}$$

or

$$\log w_p = \log \frac{\mu w}{1-\alpha} + (1-\alpha) \log N \tag{4.3}$$

Eq. 4.3 indicates that a plot of log w_p versus log N results in a straight line, as shown in Figure 4.3. The slope of the straight line, S, is $1-\alpha$ or

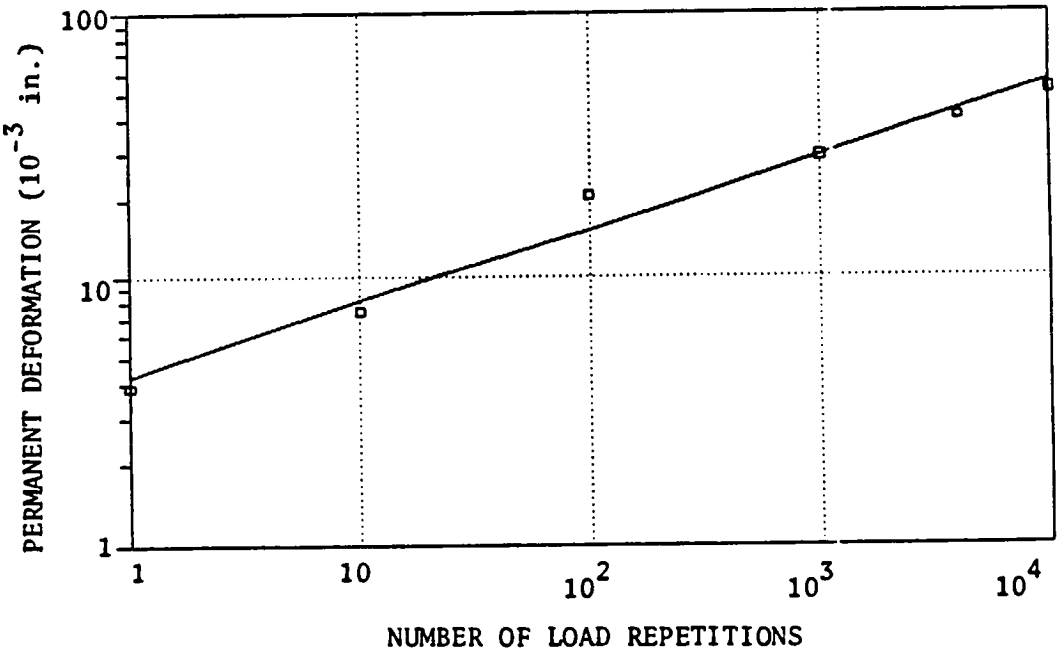

Figure 4.3 Log-log plot of deformation versus number of repetitions (1 in. = 25.4 mm)

$$\alpha = 1 - S \tag{4.4}$$

The intercept at N=1 is $I = \mu w/(1-\alpha)$ or

$$\mu = \frac{I\ S}{w} \tag{4.5}$$

The permanent deformation parameters, α and μ, of the small scale model were determined from Eqs. 4.4 and 4.5 and compared with those by VESYS.

Permanent Strains

Although permanent strains were measured under both repeated and static loads, only those under the static load are presented in this report. The correction of permanent strains for the applied load is similar to those of permanent deformations. Similar to permanent deformations, permanent strains were also smoothed out by nonlinear regression.

4.5 Presentation and Discussion of Test Results

The final reduced data for 10g, 20g and 1g tests are presented in Tables 4.3, 4.4 and 4.5, and those for the static load tests in Tables 4.6 and 4.7. Note that some specimens had only one test, while the others had several tests. If more than one tests were made on the same specimen, the average results were used. The thicknesses and deformations shown in the tables have all been scaled back to the prototype by multiplying the 1:10 model by 10 and the 1:20 model by 20. The results are presented as a series of bar charts and discussed below.

Comparison between 10g and 20g Repeated Load Tests

The most important part of this research is to verify the "modeling of models" concept by comparing the 1:10 and 1:20 models. A comparison of the overall averages between 10g and 20g tests, as shown in Tables 4.3 and 4.4,

Table 4.3 Results of 10g Tests

Specimen No.	Prototype Thickness (in.)	Density (pcf)	Resilient Strain 10^{-6} in./in.	Resilient Deformation 10^{-3} in.	Prototype Permanent Deformation (10^{-3} in.) Number of Repetitions						Permanent Deformation Parameters	
					1	10	100	1000	4000	10000	α	μ
08.200	10.08	144.0	226.0	7.4	13.25	23.82	42.84	77.06	109.72	138.58	0.745	0.454
08.300	9.90	143.4	195.5	8.8	10.43	15.74	23.76	35.86	45.95	54.13	0.821	0.210
07.200	10.36	139.3	175.1	6.7	7.89	16.24	33.42	68.75	106.16	141.46	0.687	0.369
07.200	10.36	139.3	159.4	6.3	10.82	15.58	22.44	32.31	40.25	46.54	0.842	0.270
AVERAGE			167.2	6.5	9.35	15.91	27.93	50.53	73.2	94.00	0.764	0.321
07.300	10.06	142.2	202.7	2.9	25.36	34.09	45.83	61.59	73.59	82.79	0.872	1.120
07.300	10.06	142.2	194.6	7.5	9.68	22.13	50.61	115.73	190.43	264.66	0.641	0.466
07.300	10.06	142.2	200.4	8.4	11.06	16.32	24.08	35.53	44.91	52.43	0.831	0.223
AVERAGE			199.2	6.3	15.37	24.18	40.17	70.95	102.97	133.29	0.781	0.604
OVERALL AVERAGE	10.10	142.2	197.0	7.2	11.72*	18.61*	30.62*	52.45*	74.04*	93.81*	0.778	0.397

*Not including 08.200, 1 in. = 25.4 mm, 1 pcf = 157.1 N/m^3

Table 4.4 Results of 20g Tests

Specimen No.	Prototype Thickness (in.)	Density (pcf)	Resilient Strain 10^{-6} in./in.	Resilient Deformation 10^{-3} in.	Prototype Permanent Deformation (10^{-3} in.) Number of Repetitions						Permanent Deformation Parameters	
					1	10	100	1000	4000	10000	α	μ
H8.200	10.62	144.3	148.3	7.6	14.95	35.88	86.07	206.51	349.75	495.45	0.619	0.744
H8.300	9.62	145.6	189.8	8.4	12.87	22.06	37.80	64.79	89.62	111.05	0.766	0.360
H7.200	10.66	139.7	169.3	4.2	11.21	18.72	31.25	52.17	71.02	87.09	0.777	0.599
H7.200	10.66	139.7	170.3	8.1	8.19	13.47	22.16	36.45	49.18	59.96	0.784	0.220
AVERAGE			169.8	6.2	9.69	16.09	26.70	44.31	60.10	73.52	0.781	0.409
H7.300	10.26	139.3	166.9	2.6	5.99	12.31	25.31	52.01	80.26	106.90	0.687	1.715
H7.300	10.26	139.3	180.9	4.6	15.52	26.16	44.09	74.32	101.78	125.28	0.758	0.817
H7.300	10.26	139.3	188.7	4.1	10.34	17.36	29.13	48.90	66.79	82.07	0.775	0.568
H7.300	10.26	139.3	177.5	2.6	7.32	13.25	23.99	43.43	62.08	78.62	0.742	0.712
AVERAGE			178.5	3.5	9.79	17.27	30.63	54.66	77.72	98.22	0.744	0.689
OVERALL AVERAGE	10.29	142.2	171.6	6.4	7.56*	18.47*	31.71*	54.59*	75.84*	94.26*	0.728	0.551

*Not including H8.200, 1 in. = 25.4 mm, 1 pcf = 157.1 N/m^3

Table 4.5 Results of 1g Tests

Specimen No.	Prototype Thickness (in.)	Density (pcf)	Resilient Strain 10^{-6} in./in.	Resilient Deformation 10^{-3} in.	Prototype Permanent Deformation (10^{-3} in.) Number of Repetitions						Permanent Deformation Parameters	
					1	10	100	1000	4000	10000	α	μ
H8.200	10.62	144.3	372.0	41.5	2.46	7.53	23.05	70.59	138.5	216.22	0.514	0.029
H8.300	9.62	145.6	436.1	35.8	18.42	41.85	95.07	215.96	353.92	490.57	0.644	0.180
H7.200	10.66	139.7	312.3	34.7	13.71	36.57	97.53	260.11	469.52	693.72	0.574	0.168
H7.300	10.26	139.3	238.5	21.8	6.62	14.64	32.38	71.63	115.52	158.43	0.655	0.104
H7.300	10.26	139.3	272.5	27.1	26.51	54.12	110.47	255.51	346.54	460.35	0.690	0.303
AVERAGE			255.5	24.4	16.56	34.38	71.42	148.57	231.03	309.39	0.672	0.203
OVERALL AVERAGE	10.29	142.2	344.0	34.1	16.23*	37.60*	88.01*	208.21*	351.49*	497.89*	0.601	0.145

*Not including H8.200, 1 in. = 25.4 mm, 1 pcf = 157.1 N/m^3

Table 4.6 Results of Static Load Tests on 1:10 Models

Specimen No.	Type of Response	Loading Time (sec)										
		0.01	0.03	0.1	0.3	1	3	10	30	100	300	1000
08.200	Deformation (10^{-3} in.)	3.70	8.02	14.91	22.09	29.18	33.86	36.86	38.34	39.88	42.58	49.08
	Strain (10^{-6} in./in.)	40.25	97.26	196.98	306.79	417.26	487.48	525.71	536.10	541.28	560.71	625.82
08.300	Deformation (10^{-3} in.)	0.34	1.65	5.51	11.24	17.60	21.19	22.26	21.91	22.07	24.62	34.01
	Strain (10^{-6} in./in.)	39.22	94.17	191.47	301.30	416.11	493.24	538.91	553.02	556.77	568.45	614.22
07.200	Deformation (10^{-3} in.)	0.81	2.60	6.57	11.63	17.17	20.85	23.01	23.93	25.16	27.99	35.77
	Strain (10^{-6} in./in.)	101.35	173.56	276.38	383.03	500.29	596.70	683.84	746.48	802.95	853.09	921.33
07.300	Deformation (10^{-3} in.)	5.73	7.65	10.26	13.13	16.78	20.52	24.92	29.02	33.37	36.93	40.08
	Strain (10^{-6} in./in.)	114.57	179.89	266.48	351.97	443.42	518.08	586.56	637.53	685.46	728.82	786.36
Overall Average	Deformation (10^{-3} in.)	2.65	4.98	9.31	14.52	20.18	24.11	26.76	28.30	30.12	33.03	39.74
	Strain (10^{-6} in./in.)	73.85	136.22	232.83	335.77	444.27	523.88	583.76	618.28	646.62	677.77	736.93

Note: 1 in. = 25.4 mm

Table 4.7 Results of Static Load Tests on 1:20 Models

Specimen No.	Type of Response	Loading Time (sec)										
		0.01	0.03	0.1	0.3	1	3	10	30	100	300	1000
H8.200	Deformation (10^{-3} in.)	1.51	4.08	8.96	14.61	20.46	24.22	26.34	27.10	27.89	29.87	35.47
	Strain (10^{-6} in./in.)	39.10	97.05	201.81	320.93	444.76	526.34	572.73	585.78	589.64	605.34	664.08
H8.300	Deformation (10^{-3} in.)	0.71	2.62	7.17	13.05	19.06	22.29	23.14	22.58	22.16	23.40	28.89
	Strain (10^{-6} in./in.)	71.33	138.33	231.47	315.69	386.56	423.95	439.97	443.67	451.96	479.15	554.93
H7.200	Deformation (10^{-3} in.)	2.37	3.67	5.55	7.69	10.39	13.05	15.94	18.34	20.48	21.82	22.53
	Strain (10^{-6} in./in.)	109.92	187.62	292.76	394.16	495.82	571.07	632.92	676.33	721.84	776.11	871.85
H7.300	Deformation (10^{-3} in.)	4.59	6.10	7.95	9.74	11.71	13.44	15.21	16.67	18.09	19.27	20.47
	Strain (10^{-6} in./in.)	109.39	178.84	277.15	381.15	500.40	604.38	704.67	780.33	847.02	897.83	951.12
Overall Average	Deformation (10^{-3} in.)	2.30	4.12	7.41	11.27	15.41	18.25	20.16	21.17	22.16	23.59	26.84
	Strain (10^{-6} in./in.)	82.44	150.46	250.80	352.98	456.89	531.44	587.57	621.53	652.62	689.61	760.50

Note: 1 in. = 25.4 mm

indicates that both tests check very well for every response except for the permanent deformation parameter μ, which exhibits a large range of variations. The resilient strain and deformation of the 10g test are slightly greater than those of the 20g test, probably due to the better contact condition between the asphalt layer and the subgrade in the 20g tests.

Resilient Strains

The resilient strain at the bottom of asphalt layer causes the fatigue cracking of the asphalt mixture and is an important factor for pavement design. Figure 4.4 shows the resilient strains for all test combinations. The letter O implies an one inch asphalt specimen for the 10g test, while the letter H implies a half inch specimen for the 20g test. The first four sets of bars compare 10g and 20g tests for each pair of specimens with the same

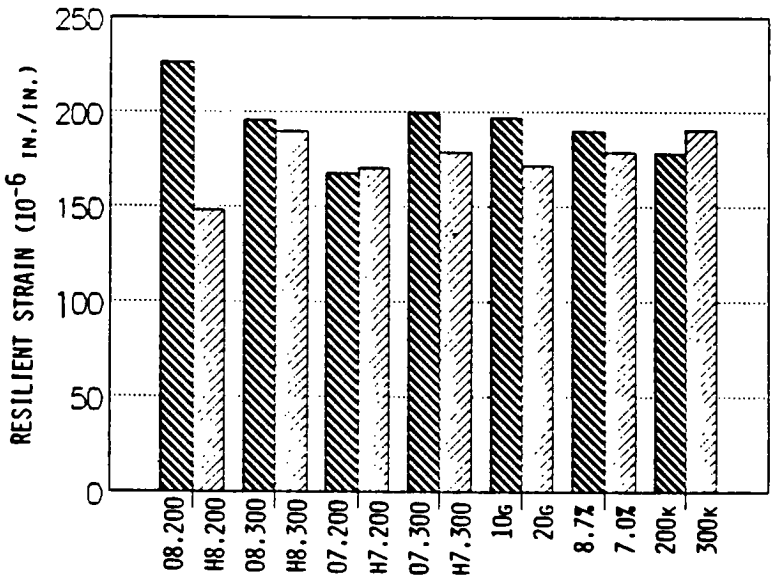

Figure 4.4 Comparison of resilient strains between 10g and 20g tests

asphalt content and compaction level, while the last three sets of bars show the average values. Although emphasis is placed on the comparison between 10g and 20g tests, comparisons between asphalt contents of 8.7 versus 7% and compaction levels of 200 versus 300 kip can also be easily seen from the average on the right side of the figure. The figure shows that the 10g tests check well with the 20g tests and that the two asphalt contents and two levels of compaction have very small effects on resilient strains.

Resilient Deformations

Figure 4.5 shows the resilient deformations on the pavement surface for all test combinations. The resilient deformation is important because the permanent deformation is proportional to the resilient deformation, as indicated by Eq. 4.1. To determine the permanent deformations, a knowledge of

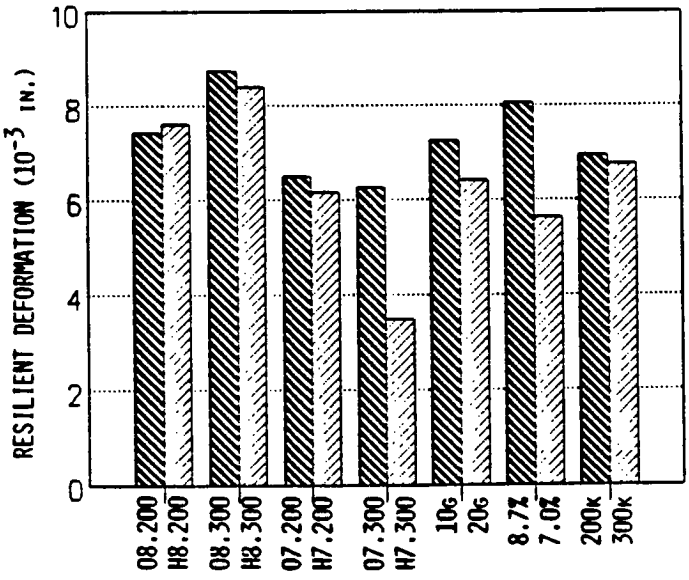

Figure 4.5 Comparison of resilient deformations between 10g and 20g tests (1 in. = 25.4 mm)

resilient deformation is required. The permanent deformation parameter, μ, is determined from the resilient deformation, as indicated by Eq. 4.5. The figure shows that, except for specimens 7.300, the resilient deformations obtained from 10g and 20g tests check reasonably well, although the values from the 10g tests appear to be slightly larger than those from the 20g tests. The fact that both resilient strains and deformations are smaller in the 20g tests is due to the better contact between the asphalt layer and the subgrade, as will be explained later. The figure also shows that the resilient deformations are about the same for the two compaction levels but asphalt content of 8.7% has greater resilient deformations than that of 7%. This may indicate that asphalt contents have more effect on resilient deformations than on resilient strains.

Permanent Deformations

Figure 4.6 shows the permanent deformations on the pavement surface. The four horizontal lines in each bar indicate the permanent deformations at 1, 10, 100 and 1,000 repetitions, respectively. The top of the bar indicates the permanent deformation at 10,000 repetitions. In the figure, only the average for the 10g and 20g tests is shown. It can be seen that permanent deformations have a large range of variations, particularly at the later part of the test when the number of repetitions are large. The very large permanent deformations for specimen H8.200 are totally unreasonable and, together with O8.200, were not used to determine the average. Inspite of the large variability, the average permanent deformations between 10g and 20g tests also check quite well.

Figures 4.7 and 4.8 show the permanent deformation parameters, α and μ, for all test combinations. There are not much variations in α but large variations in μ among the tests. No explanation can be made why the values of μ for 10g tests are consistently smaller than those for the 20g tests. In view of the large variations between replicated tests, the difference in μ between 10g and 20g tests should not be considered significant.

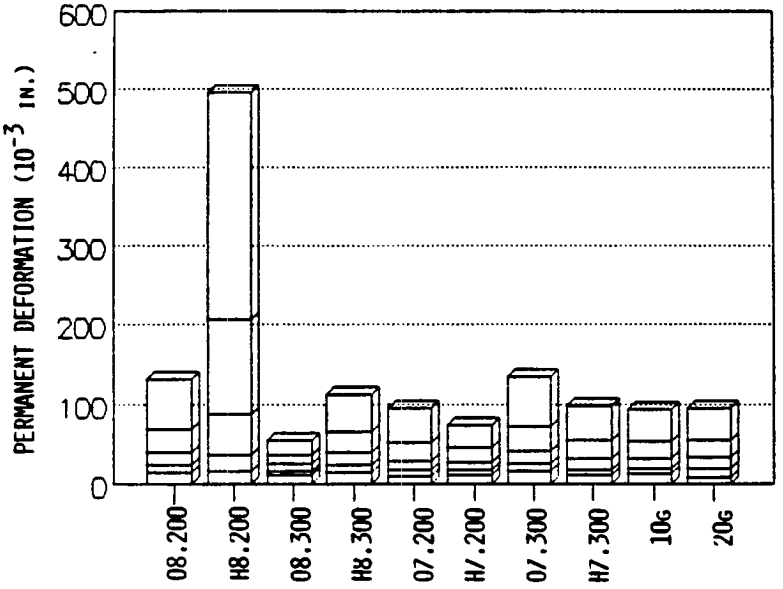

Figure 4.6 Comparison of permanent deformations between 10g and 20g tests (1 in. = 25.4 mm)

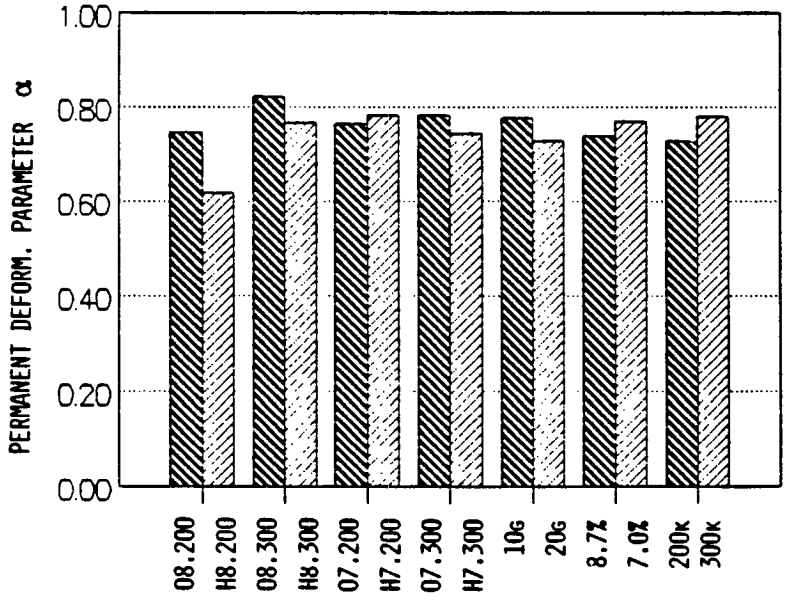

Figure 4.7 Comparison of α between 10g and 20g tests

The inconsistency on the computed value of μ is because it depends on three factors,I, S, and w, as indicated by Eq. 4.5. Note that I is the permanent deformation at the first load repetition, S is the slope of the log-log plot of permanent deformation versus number of repetitions, and w is the resilient deformation on the pavement surface. Table 4.8 shows the values of w, I, α, and S for specimens O8.300 and H8.300 as well as the computed μ. These values can be found in Tables 4.3 and 4.4 but are presented here for comparison. It should be pointed out that $S = 1 - \alpha$, as indicated by Eq. 4.4, and that the values of μ shown in Table 4.8 are slightly different from those in Tables 4.3 and 4.4 due to the round off error.

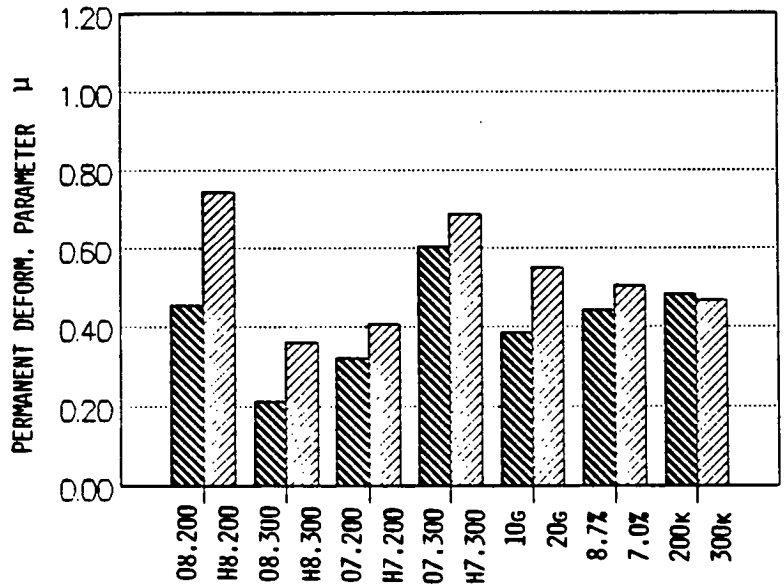

Figure 4.8 Comparison of μ between 10g and 20g tests

Table 4.8 Comparison of Parameters Affecting Permanent Deformations

Specimen No.	w (10^{-3} in.)	I (10^{-3} in.)	α	S	μ
O8.300	8.8	10.43	0.821	0.179	0.212
H8.300	8.4	12.87	0.766	0.234	0.358

Note: 1 in. = 25.4 mm

It is interesting to note that the values of w, I, and α appear to be quite consistent. However, when converted into S and μ, a large difference between the two specimens exists.

Comparison between 1:10 and 1:20 Models under Static Load

After the completion of the repeated load test, a 1,000 sec creep test was performed on the same specimen. The parameters to be compared are the vertical deformations on the surface and the radial tensile strains at the bottom of asphalt layer as a function of time. A comparison of the overall average between 1:10 and 1:20 models, as shown in Tables 4.6 and 4.7, indicates that both models check very well. The deformations of the 1:10 models are somewhat larger than the 1:20 models, probably due to the better contact condition in the 1:20 models.

Deformation

Figure 4.9 shows the deformations on the pavement surface at various times. The five sections of each bar indicate the accumulated deformations at 0.1, 1, 10, 100 and 1,000 sec. The deformations of the 1:20 model appear to be smaller than those of the 1:10 model, probably due to the better contact between the asphalt layer and the subgrade. The 8.7% asphalt content has deformations slightly greater than the 7% and the 200 kips slightly greater than the 300 kips. Due to the variability of the tests, these differences should not be considered significant.

Strains

Figure 4.10 shows the tensile strains at the bottom of asphalt layer. The strains are much more consistent compared to the deformations. The strains in the 1:10 model check very closely with those in the 1:20 model for every pair of the tests. However, the 8.7% asphalt content has strains somewhat smaller than the 7 %, which is not expected.

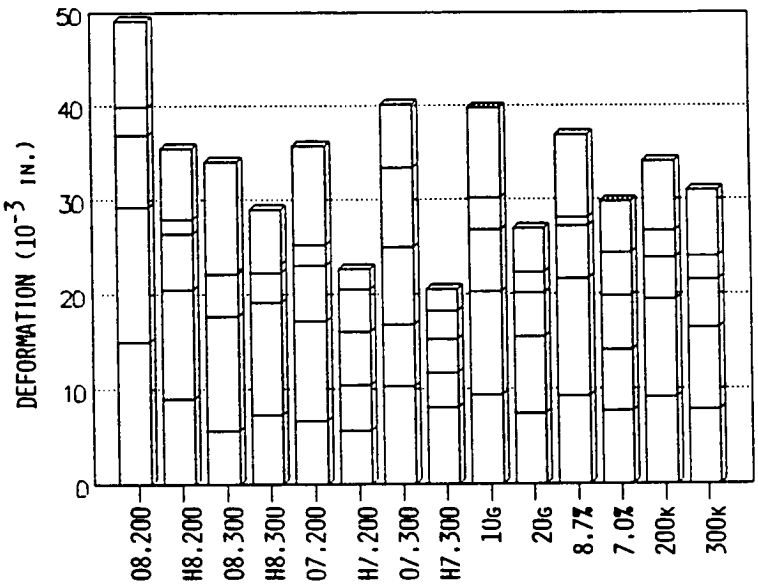

Figure 4.9 Comparison of deformations under static load between two models (1 in. = 25.4 mm)

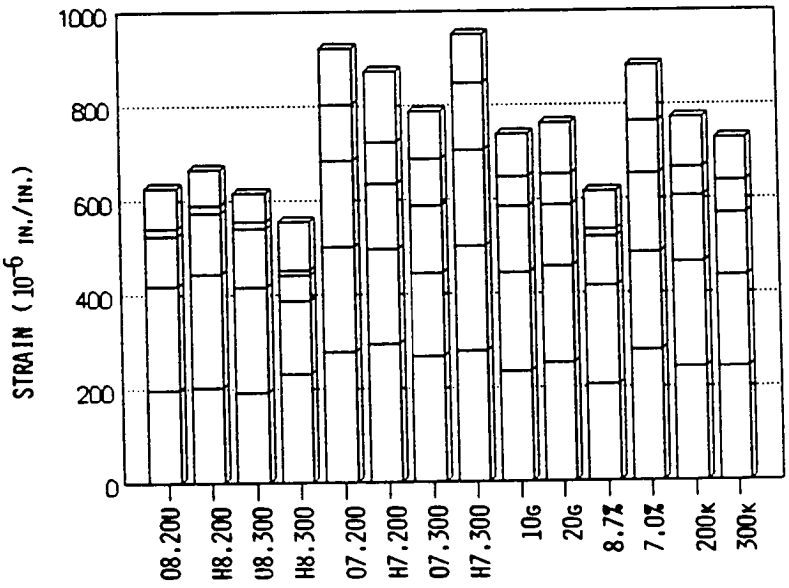

Figure 4.10 Comparison of strains under static load between two models

Comparison between 1g and 20g Tests

With the same loading and geometry, the only difference between 1g and 20g tests is the self weight, which is 20 times heavier for the 20g test. A direct comparison between 1g and 20g tests will show the effect of centrifuge on model responses. The data summarized in Tables 4.4 and 4.5 are plotted as a series of bar charts for comparison purposes.

Resilient Deformations

Figure 4.11 provides a comparison of resilient deformations between 1g and 20g tests. The resilient deformations of the 1g test are more than five times greater than those of the 20g test. A nonlinear analysis of the prototype pavement by KENLAYER indicated that a reduction of self weight to one-twentieth of the original reduced the modulus of the sand subgrade by 18% and increased the resilient deformation by only 10%. Therefore, the large difference in resilient deformations is not due to the difference in self weight but rather due to the lack of intimate contact between the

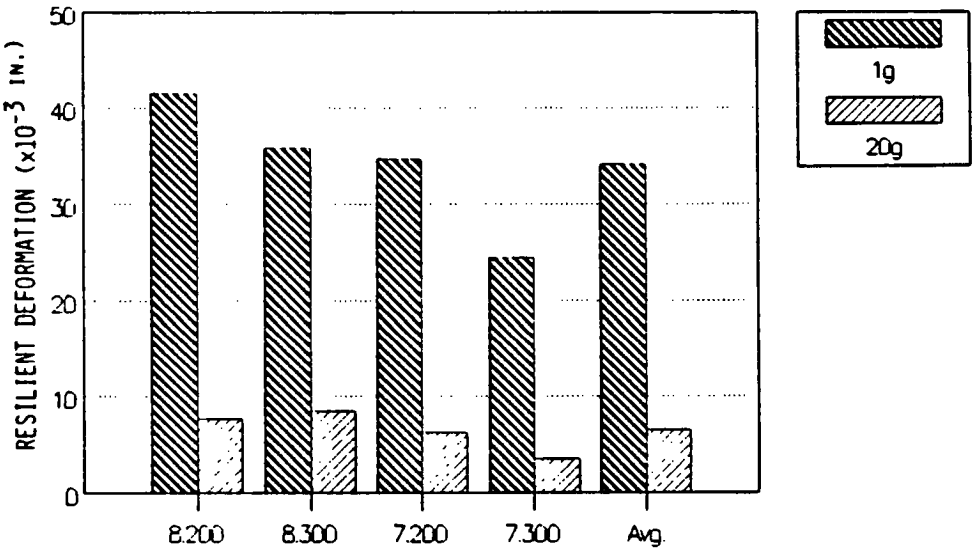

Figure 4.11 Comparison of resilient deformations between 1g and 20g tests (1 in. = 25.4 mm)

prefabricated sand asphalt and the subgrade. A very small gap between the asphalt layer and the subgrade in the 1g test will result in a large resilient deformation after multiplying by a scale factor of 20.

It was suspected that the large resilient deformation of the 1g test was due to the weaker specimen because the 1g test was performed after the 20g test. However, a rerun of the 20g test after the 1g test still arrived at the same results, indicating that the order of tests has no effect on the results obtained.

Resilient Strains

Figure 4.12 shows the resilient tensile strain at the bottom of the asphalt layer. The resilient strains of the 1g test averaged about two times greater than those of the 20g test, in contrast to the five times in resilient deformations. This is also reasonable because any gap between the asphalt layer and the subgrade will add directly to the vertical resilient deformation. However, the horizontal resilient strain is affected to a much lesser degree because the gap will be closed after the load is applied and the increase in strain is not as significant as the increase in deformation.

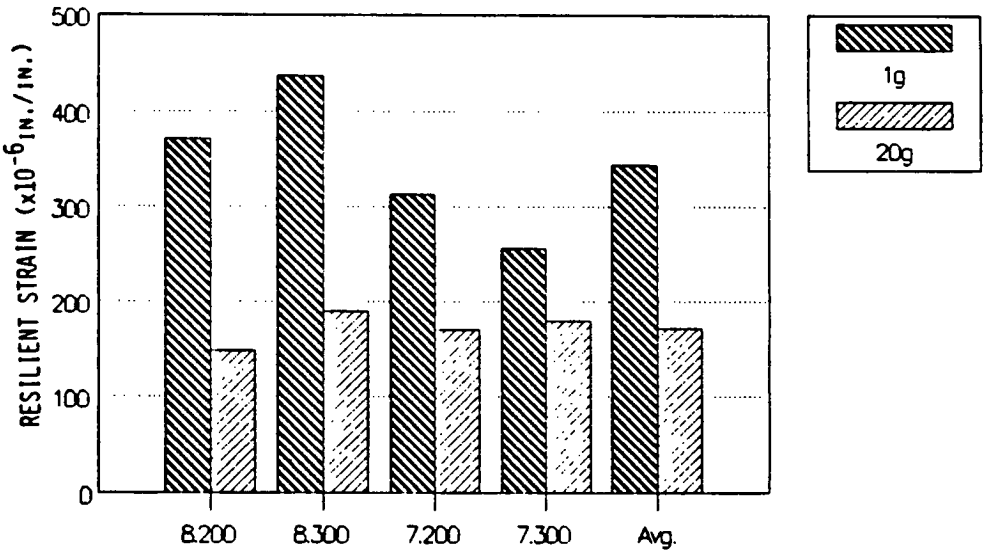

Figure 4.12 Comparison of resilient strains between 1g and 20g tests

Permanent Deformations

Figure 4.13 shows the permanent deformations on the pavement surface at 1, 10, 100 and 1,000, 10,000 repetitions. Except for specimen H8.200, the permanent deformations of the 1g model are much greater than the 20g model. The very large permanent deformations for specimen H8.200 are unreasonable and, together with O8.200, were not used in computing the average. It can be seen that the permanent deformations of the 1g test are much greater than those of the 20g test.

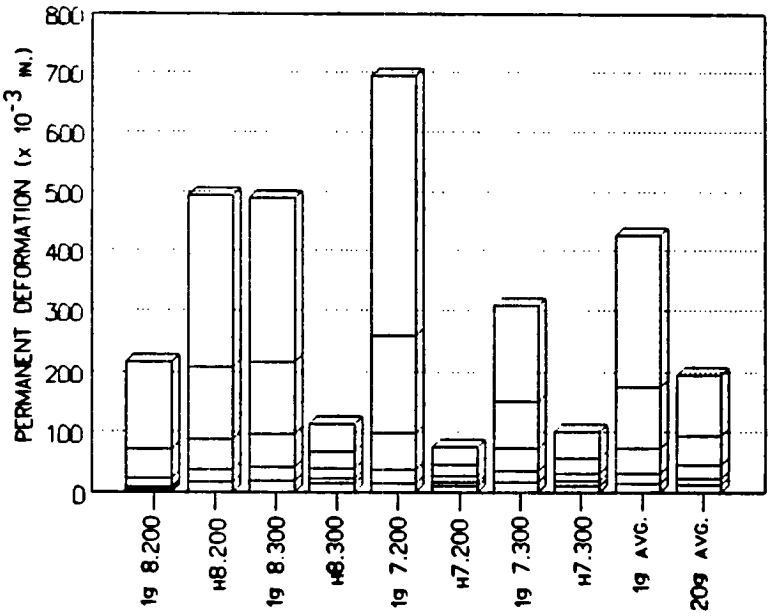

Figure 4.13 Comparison of Permanent deformations between 1g and 20g tests (1 in. = 25.4 mm)

The permanent deformation parameters, α and μ, are shown in Figures 4.14 and 4.15. The values of α for the 1g test are smaller than those of the 20g test. This is also reasonable because a smaller α indicates a weaker

pavement. The values of μ for the 1g test are much smaller than those of the 20g test because the 1g test has a much larger resilient deformation relative to the permanent deformation.

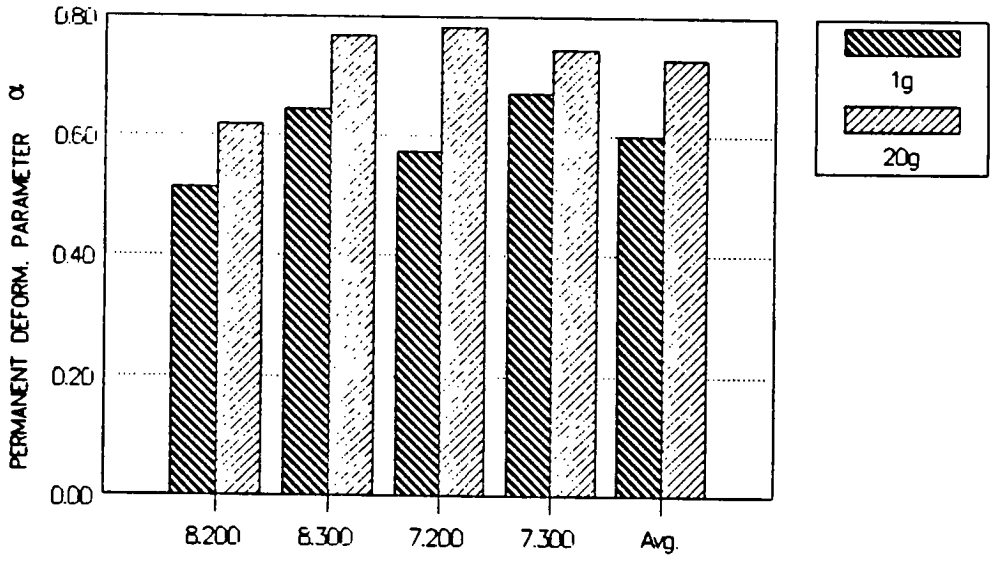

Figure 4.14 Comparison of α between 1g and 20g tests

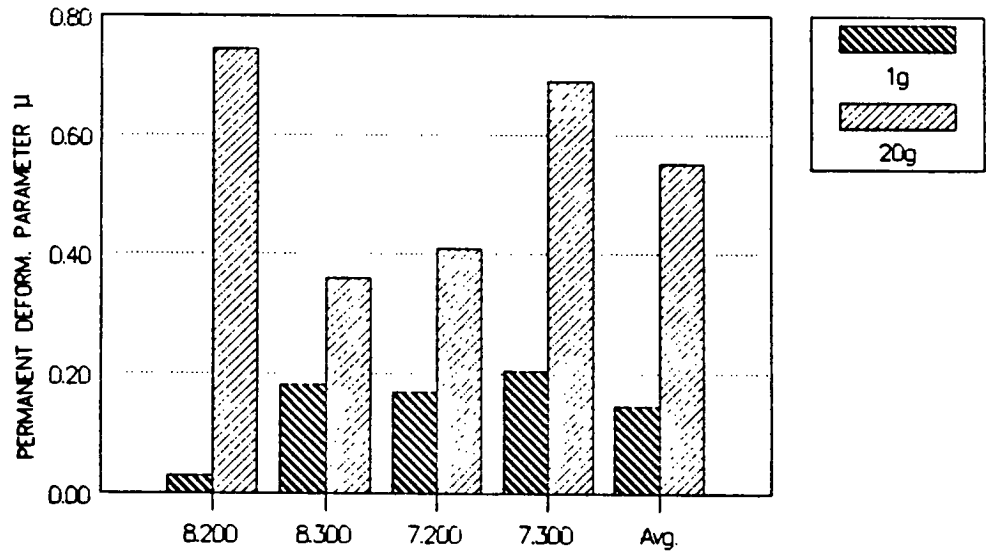

Figure 4.15 Comparison of μ between 1g and 20g tests

Chapter 5 Testing and Analysis of Cylindrical Specimens

5.1 Creep Tests of Asphalt Specimens

Two types of test were conducted on asphalt specimens: an incremental static test followed by a repeated load test. The specimens were tested at room temperature under a vertical stress of 20 psi (138 kPa) with no confining pressure. The procedures of the tests are described in the VESYS user's manual (FHWA, 1976). A 20,000 lb (89 kN) capacity electrohydraulic testing machine manufactured by the Materials Testing System (MTS) was used. Figure 5.1 shows an asphalt specimen, 4 in. (102 mm) in diameter and 8 in. (203 mm) in height, with two LVDT clamps mounted at quarter points and placed on a MTS machine.

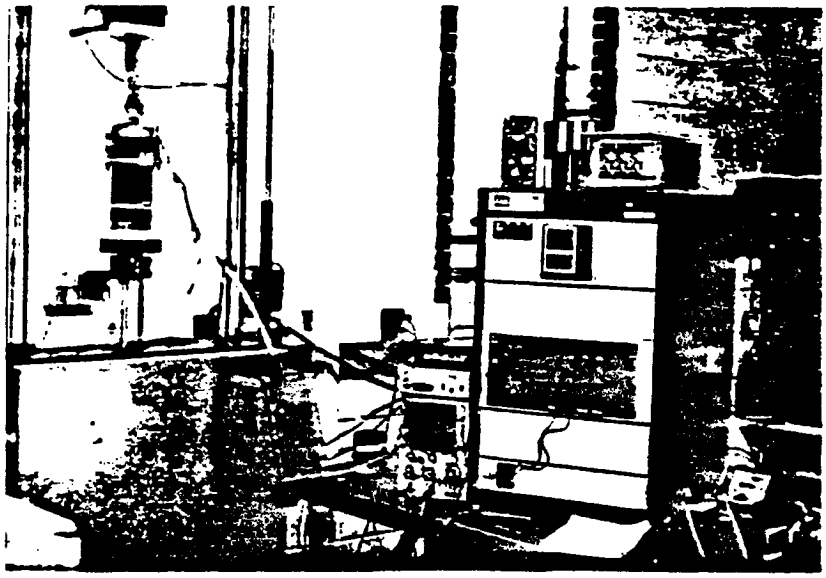

Figure 5.1 Photograph of testing asphalt specimen by MTS machine

In the incremental static test, a series of static or creep tests with duration of 0.1, 1, 10, 100 and 1,000 sec were performed to determine the permanent deformation parameters. Because the values of μ obtained from the incremental static tests experienced a wide range of variations and did not check with those from the repeated load tests, only the 1,000 sec creep test for determining the creep compliance is presented here. One possible reason for the discrepancy between the incremental static and the repeated load tests is due to the use of repeated load with a 0.45 sec loading and 0.55 sec unloading, instead of the standard haversine loading with a duration of 0.1 sec and a rest period of 0.9 sec. The repeated load test for determining the resilient modulus and permanent deformation parameters will be presented in the next section.

Analysis

The magnitude of creep deformations for the 1,000 sec creep test was monitored at 0.04, 0.1, 0.3, 1, 3, 10, 30, 100 and 1,000 sec. The deformation of specimen was considered to be zero at the start of the test.

The creep compliance, D(t), is defined as the ratio between the creep strain and the static stress and can be calculated at each time by

$$D(t) = \frac{\varepsilon(t)}{\sigma} \tag{5.1}$$

in which $\varepsilon(t)$ = axial strain at each time, t, after the application of the axial stress, σ. Note that σ is the applied load divided by the cross sectional area, or approximately 20 psi. (138 kPa) A best-fit curve of creep compliance, D(t), versus time was constructed in log-log scale. The creep compliances at 0.01, 0.03, 0.1, 0.3, 1, 3, 10, 30, 100, 300, and 1,000 sec were then obtained.

Results and Discussion

The creep compliances of all cylindrical asphalt specimens are presented

in Table 5.1. Figure 5.2 shows the creep compliances for all the specimens

Table 5.1 Creep Compliance of Cylindrical Asphalt Specimens

Specimen No	Density (pcf)	Creep Compliance (10^{-7} in.^{2}/lb) Loading Time (sec)										
		0.01	0.03	0.1	0.3	0.45	1	3	10	30	100	1000
F8.5	137.5	3.12	9.37	24.20	46.98	57.50	80.68	115.06	151.10	179.74	207.42	272.36
F8.40	145.8	3.50	4.61	7.25	12.05	14.76	22.32	39.76	72.66	117.79	177.57	231.37
F8.63	146.0	2.78	4.37	7.26	11.52	13.62	18.84	28.82	44.20	62.35	85.37	123.62
F7.20	138.9	8.53	15.24	26.24	39.98	45.97	59.18	80.24	106.89	134.41	168.68	253.76
F7.40	141.7	1.53	4.44	11.19	21.63	26.54	37.67	55.45	77.02	98.43	125.83	216.20
F7.63	143.5	2.51	4.34	7.39	11.37	13.19	17.38	24.67	35.11	47.48	65.26	119.64
M	149.0	1.11	4.36	14.09	31.84	40.78	61.67	94.90	131.83	162.45	193.33	273.16
C	147.4	0.94	4.56	16.08	38.97	49.76	73.43	106.36	136.45	158.01	182.33	298.48
VC	145.3	0.84	4.12	14.43	31.40	38.86	53.65	70.65	82.31	89.03	98.79	175.76

Note: 1 in. = 25.4 mm, 1 lb = 4.45 N, 1 pcf = 157.1 N/m^3

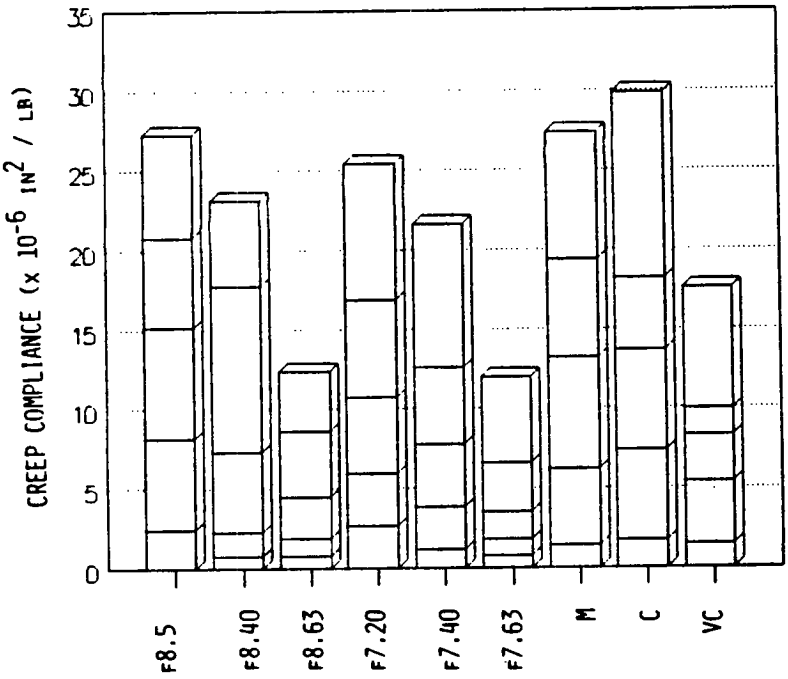

Figure 5.2 Creep compliances for all cylindrical asphalt specimens (1 in.^{2}/lb = 0.143 m^2/kN)

tested. The four horizontal lines in each bar indicate load durations of 0.1, 1, 10 and 100 sec, respectively. The top of the bar indicates the 1,000 sec duration. It can be seen from the figure that the creep compliances of fine mix decrease as the compactive level increases. The creep compliances of the medium, coarse and very coarse mixes are not very much different and fall within the range of the fine mixes. Thus the creep compliance of mixes with large aggregates can be simulated by those with smaller aggregates if the asphalt content and density of the fine mix are properly controlled.

Figure 5.3 shows a plot of creep compliances for mixtures with medium, coarse and very coarse aggregates. It can be seen that the creep compliances at the early part of the creep test are about the same for all the specimens, but the very coarse mixture over time has a lower creep compliance compared to the medium and coarse mixtures. Also shown in Figure 5.3 are the creep compliances of two fine mixes, one on the lower range and the other on the higher range.

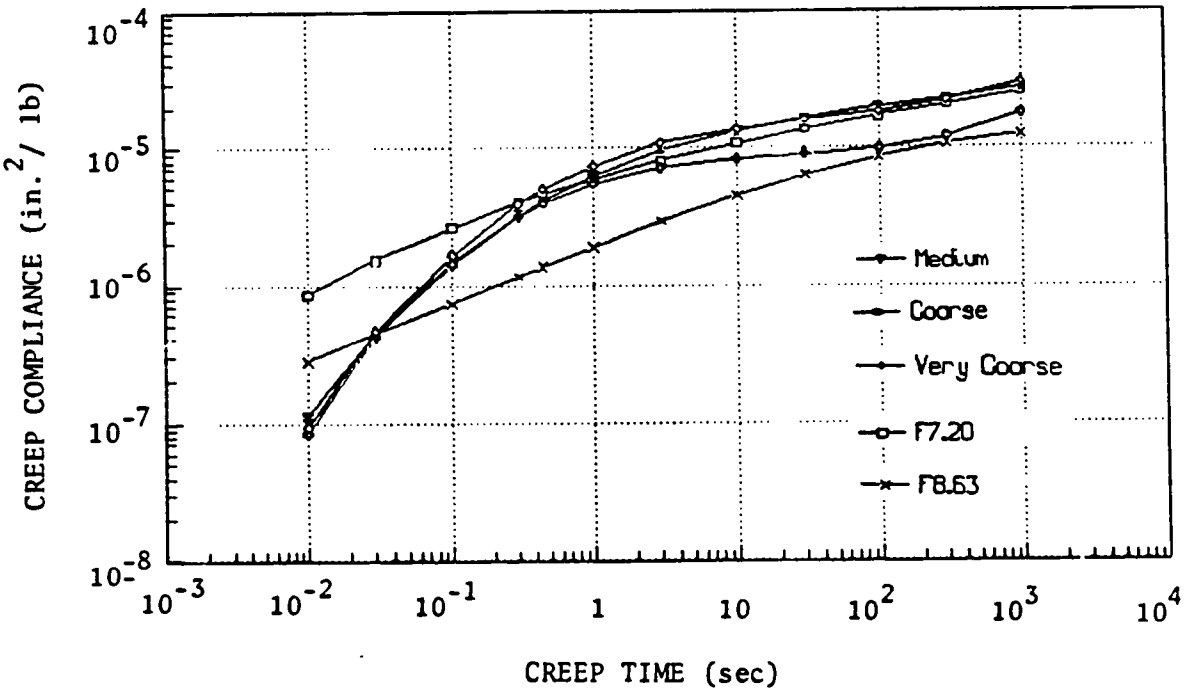

Figure 5.3 Effect of aggregate sizes on creep compliances of asphalt mixes (1 in^2/lb = 0.143 m^2/kN)

5.2 Repeated Load Tests of Asphalt Specimens

The repeated load test was performed on asphalt specimens to determine the resilient modulus and permanent deformation parameters. The test procedures are the same as those described in the VESYS user's manual (FHWA, 1976). However, the repeated compression loading was applied as a square waveform with a duration of 0.45 sec and a rest period of 0.55 sec, instead of the conventional haversine waveform with a duration of 0.1 sec and a rest period of 0.9 sec. The data acquisition setup program for this test was similar to the repeated load centrifuge test except that the channel for the strain gage was not used.

Analysis

The resilient modulus, M_R, is calculated by

$$M_R = \frac{\sigma}{\varepsilon_r} \tag{5.2}$$

in which σ = applied repeated stress, which is approximately 20 psi (138 kPa) and ε_r = resilient strain.

The permanent deformation parameters, α and μ, were calculated in the same way as for the small-scale model and can be summarized as follows:

1. The accumulated strains at 1, 10, 100, 200, 1,000, 4,000 and 10,000 repetitions were measured.

2. The log of accumulated strains is plotted against the log of repetition number. A best-fit straight line through the points was plotted. The vertical intercept at 1 repetition was denoted as I and the slope of the straight line as S.

3. The resilient strain at the 200th load repetition was calculated and denoted as e.

4. The permanent deformation properties were calculated as

$$\alpha = 1 - S \tag{5.3}$$

$$\mu = \frac{IS}{e} \tag{5.4}$$

It should be noted that α and μ are dimensionless parameters and that Eqs. 5.3 and 5.4 for the permanent deformation of cylindrical specimens are the same or in the same form as Eqs. 4.4 and 4.5 for the permanent deformation of pavement systems.

Results and Discuusion

Table 5.2 shows the results of repeated load tests on cylindrical asphalt specimens. It can be seen that the resilient modulus of fine mixes increases as the compactive level or density increases. The resilient moduli of medium, coarse and very coarse mixes all fall within the range of the fine mixes. The permanent deformation parameter, α, increases slightly as the compaction level and the size of aggregates increase.

Table 5.2 Results of Repeated Load Tests on Cylindrical Asphalt Specimens

Specimen No.	Density (pcf)	Resilient Modulus E_5 (10^3 psi)	Permanent Deformation (10^{-6} in./in.) Number of Repetitions					Permanent Deformation Parameters	
			1	10	100	1000	10000	α	μ
F8.5	137.5	2.30	77.30	146.52	277.72	526.40	997.76	0.722	0.242
F8.40	145.8	4.48	53.43	101.18	191.63	362.93	687.36	0.723	0.381
F8.63	146.0	5.21	24.43	39.25	63.05	101.27	162.66	0.794	0.146
F7.20	138.9	3.71	33.57	73.17	159.46	374.53	757.40	0.662	0.197
F7.40	141.7	4.83	28.44	54.51	104.45	200.17	383.60	0.718	0.231
F7.63	143.5	8.68	15.10	27.43	49.82	90.48	164.32	0.741	0.185
M	149.0	3.25	51.24	97.62	185.99	354.36	675.16	0.720	0.247
C	147.4	5.17	54.95	98.61	176.98	317.62	570.02	0.746	0.399
VC	145.3	3.57	59.13	94.55	151.17	241.70	386.45	0.796	0.257

Note: 1 psi = 6.9 kPa, 1 pcf = 157.1 N/m^3

Figure 5.4 shows the effect of aggregate size on permanent strains under repeated load tests. At the initial stage of the test, the permanent strains are nearly the same. However, at the later stage, the permanent strain decreases as the size of aggregates increases. Also shown in Figure 5.4 are the permanent strains of two fine mixes which are the upper and lower bounds of all tests.

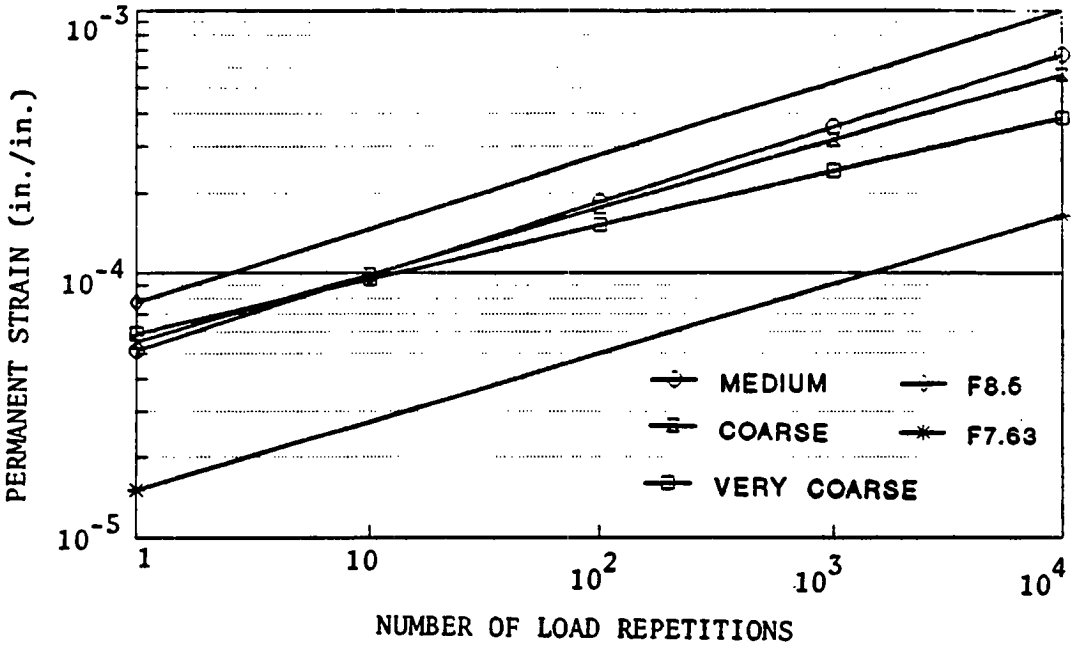

Figure 5.4 Effect of aggregate sizes on permanent strains of asphalt mixes

5.3 Sand Specimens

The sand specimens were subjected to 10,000 repetitions in the permanent deformation test, followed by a 1,000 sec creep test. The test procedures and methods of analysis are the same as described for asphalt specimens except that a confining pressure of 1.16 psi (8 kPa) and a static or repeated deviator stress of 3 psi (21 kPa) were employed. The use of these stresses was based on the actual vertical and radial stresses in the prototype pavement, as computed by KENLAYER. The creep test was used to determine the creep compliance, D(t), while the repeated load test to determine the permanent deformation parameters, α and μ. To find the relationship between the resilient modulus and the state of stresses, a resilient modulus test with variable confining pressures and deviator stresses was also performed after the creep test.

Specimen Preparation

The sand specimens were 4 in. (102 mm) in diameter and 8 in. (203 mm) in height. The procedures for specimen preparation are listed below:

1. A porous stone, 4 in. (102 mm) in diameter, was placed on the bottom platen to which a thin layer of vacuum grease was applied.
2. A rubber membrane was stretched inside a split mold by overlapping at both ends. A vacuum was then applied between the mold and the membrane to keep the membrane against the mold.
3. The mold with the membrane was slid over the porous stone and part of the bottom platen. The mold was supported at the bottom by three temporary blocks to make sure that the mold is vertical.
4. A predetermined amount of sand, based on a density of 105 pcf, was poured into the mold in 5 layers, each rodded 25 times with a steel rod.
5. The surface of the sand was leveled and a porous stone was placed on top followed by a greased platen.
6. The membrane was rolled over both the top and bottom platens and a vacuum was applied to the specimen through a hole in the bottom platen.
7. The mold was removed. Two O rings were placed around the top and bottom platens by a membrane stretcher.
8. The diameter and height of the specimen were measured.
9. A triaxial cell was installed.
10. The cell was filled partially with water and compressed air was applied to the water.
11. The vacuum was removed and a LVDT was attached to the loading piston outside the triaxial chamber.

Figure 5.5 is a schematic diagram of the setup. When an air pressure of 1 psi (7 kPa) was used, the actual confining pressure was 1.16 psi (8 kPa) because the average pressure due to the weight of water in the chamber was about 0.16 psi (1.1 kPa).

Permanent Deformation Parameters

A repeated load test with a 0.45 sec loading and a 0.55 sec rest period

was used to determine the permanent deformation parameters, α and μ, of the sand specimen. The method of analysis is the same as that for the cylindrical asphalt specimens and will not be described here.

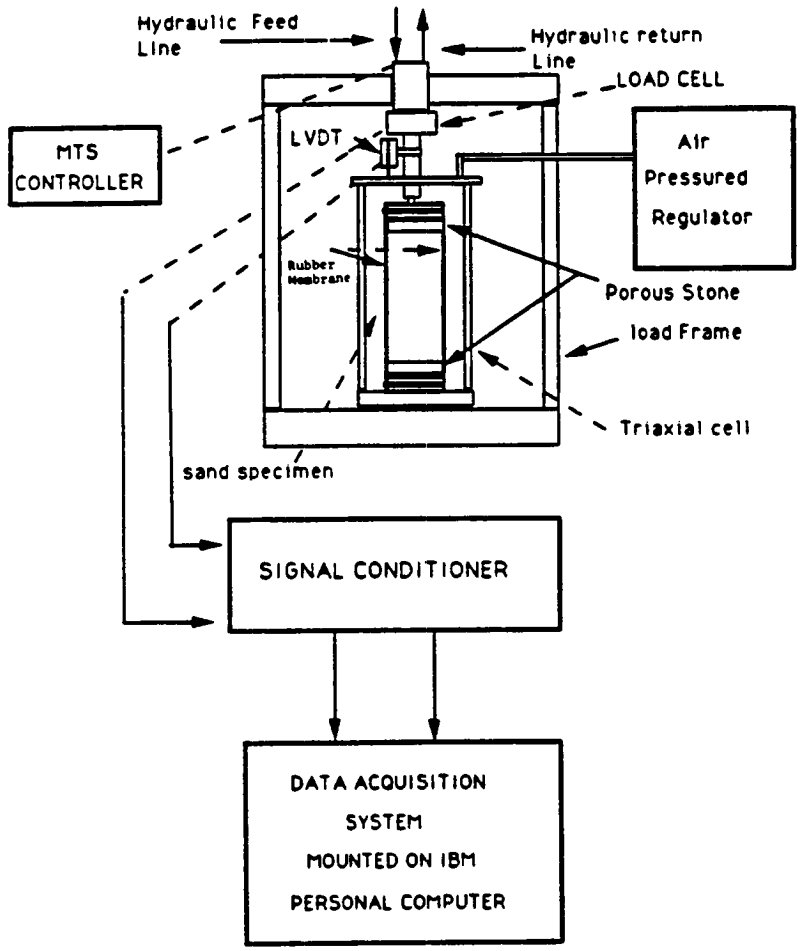

Figure 5.5 A schematic diagram of test setup for sand specimen

Table 5.3 is a summary of the repeated load test results. The permanent deformation parameters, α and μ, were computed from the resilient modulus and permanent strains by Eqs. 5.3 and 5.4 and used later as input to the VESYS computer program.

Table 5.3 Results of Repeated Load Test on Cylindrical Sand Specimen

Resilient Modulus at at 200th Repetition (10 psi)	Permanent Strain (10^{-6} in./in.) Loading Time (sec)					Permanent Deformation Parameter	
	1	10	100	1000	10000	α	μ
2.03	9.96	14.39	20.79	30.02	43.00	0.84	0.009

Note: 1 psi = 6.9 kPa

Creep Test

The 1,000 sec creep test was conducted to determine the creep compliance of the sand specimen. The method of analysis is the same as that for cylindrical asphalt specimens.

Table 5.4 is a summary of the creep test results. The creep compliances of the asphalt mixture and the sand were used as input to the KENLAYER computer program to determine the responses of the prototype pavement under a static load. Note that the compliances at longer loading times fluctuate somewhat due to nonlinear regression.

Table 5.4 Creep Compliance of Cylindrical Sand Specimen

Creep Compliance (10^{-7} in.^{2}/ lb) Loading Time (sec)										
0.01	0.03	0.1	0.3	1	3	10	30	100	300	1000
24.32	160.67	450.15	635.96	663.13	621.13	597.18	626.61	707.88	766.48	663.13

Note: 1 in.^{2}/lb = 0.143 m^2/kN

Resilient Modulus

The resilient modulus test was conducted to determine the coefficient, K_1, and exponent, K_2, of the sand. A load frequency of 1 Hz with a 0.45 sec loading and 0.55 sec rest period was used. This frequency was the same as that used in the centrifuge test.

The test applied various combinations of deviator stress and confining pressure to the specimen, each for 200 load repetitions. The sequence of stress applications is shown in Table 5.5. The first 1,200 repetitions are for specimen conditioning. The data collection started at a confining pressure of 6 psi (41 kPa), which was then reduced to 4, 2 and 1 psi. (28, 14 and 7 kPa) For each confining pressure, the deviator stress was increased after every 200 repetitions.

The relationship between the resilient modulus and the state of stresses can be expressed as

$$M_R = K_1 (\theta)^{K_2} \tag{5.5}$$

in which θ = bulk stress or the sum of the principal stresses; K_1, K_2 = material constants. The results of resilient modulus test are plotted in Figure 5.6. The slope of the straight line shown in the figure is K_2 and the intercept at a bulk stress of 1 psi (7 kPa) is K_1. The equations for the resilient modulus are

$$M_R = 7940\ \theta^{0.34} \tag{5.6}$$

Seed et al. (1965) reported K_1 of 6700 and K_2 of 0.36 for sand, which check well with Eq. 5.6.

Table 5.5 Sequences of Stresses for Resilient Modulus Tests of Sand

Phase	Repetitions	Deviator Stress (psi)	Confining Pressure (psi)
Specimen Conditioning	200	1.5	1.5
	200	3.0	1.5
	200	3.0	3.0
	200	4.5	3.0
	200	4.5	4.5
	200	6.0	4.5
Data Collection	200	2.0	6.0
	200	4.0	6.0
	200	6.0	6.0
	200	8.0	6.0
	200	12.0	6.0
Data Collection	200	1.0	4.0
	200	2.0	4.0
	200	4.0	4.0
	200	6.0	4.0
	200	8.0	4.0
Data Collection	200	1.0	2.0
	200	2.0	2.0
	200	4.0	2.0
	200	6.0	2.0
Data Collection	200	1.0	1.0
	200	2.0	1.0
	200	4.0	1.0

Note: 1 in. = 25.4 mm

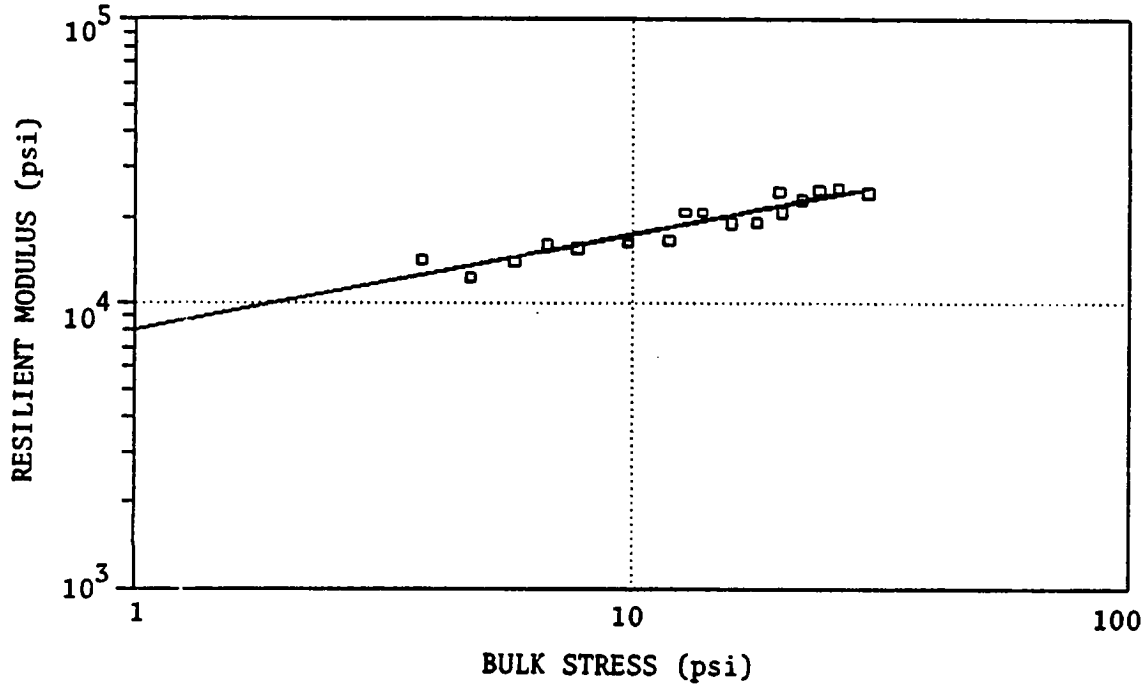

Figure 5.6 Resilient modulus for sand specimen based on bulk stresses (1 psi = 6.9 kPa)

Chapter 6 Comparison between Centrifuge and Computer Models

6.1 Computer Input

Two computer models were used to determine the deformations and strains in the prototype pavement. KENLAYER is a comprehensive computer program with linear elastic, nonlinear elastic and linear viscoelastic options for determining the resilient modulus of the sand subgrade under repeated loads, as well as the vertical resilient deformation at the pavement surface and the radial resilient strain at the bottom of asphalt layer. VESYS is a linear computer program and can be used to determine the permanent deformations based on the resilient modulus of the sand layer obtained by KENLAYER. Both programs can be used to determine the deformations and strains under static loads.

In view of the fact that the responses of the various models with scale factors of 1:10 and 1:20, asphalt contents of 8.7 and 7%, and compaction levels of 200 and 300 kips are not very much different, the average responses of the above eight cases were used to represent the centrifuge results. The comparisons were made on both repeated and static loadings.

Geometry and Loading

The prototype Pavement to be analyzed by the computer models is a three-layer system consisting of an asphalt layer with a thickness of 10.2 in. (259 mm), which is the average thickness of the centrifuge specimens after being scaled back to the prototype, a sand layer with a thickness of 30 in. (762 mm) and a rigid base with an elastic modulus of 10^{10} psi, which can be considered as infinity. The load is applied to the layered system over a

circular loaded area with a radius of 6 in. (151 mm). The intensity of the load is 80 psi (552 kPa) for the repeated load and 90 psi (621 kPa) for the static load. The 90 psi (621 kPa) load was also used in KENLAYER to determine the elastic modulus of the sand, based on the geostatic and loading stresses at the midheight of the sand layer under the center of the loaded area. The geostatic stresses due to self weight were based on unit weights of 143 pcf (22.5 kN/m^3) for asphalt layer and 105 pcf (16.5 kN/m^3) for sand and a coefficient of earth pressure at rest, K_o, of 0.4. Because the computer models give the deformation at the center of a flexible plate while the centrifuge models apply the load over a rigid plate, the deformations obtained from computer models must be multiplied by a factor of $\pi/4$, or 0.785 (Timoshenko and Goodier, 1951). The above factor is based on a homogeneous half space and may not be exact for a layered system. However, the error is believed to be small and a factor of 0.785 was also recommended by Yoder and Witczak (1975) for use in layered systems.

Properties of Asphalt Mixtures

The properties of asphalt mixtures to be determined include the resilient modulus and the permanent deformation parameters, α and μ, under repeated loading and the creep compliance under static loading. A Poisson's ratio of 0.35 was assumed for the asphalt layer.

Table 6.1 shows the computation of resilient modulus and permanent deformation parameters for computer input. The properties for specimens F8.5, F8.40, F7.20 and F7.40 were obtained from repeated load tests on cylindrical specimens, as presented in Chapter 5. The average density for centrifuge specimens with an asphalt content of 8.7% was 144.3 pcf (22.7 kN/m^3) and that with an asphalt content of 7% was 140.1 pcf (22.0 kN/m^3). The properties for each asphalt content were obtained by a straight line interpolation and the average values were used to represent the properties of the asphalt layer. The same method was used to compute the creep compliance as shown in Table 6.2.

Table 6.1 Properties of Fine Asphalt Mixtures for Computer Input

Specimen No.	Density (pcf)	Resilient Modulus (10^5 psi)	Permanent Deformation α	μ
F8.5	137.5	2.30	0.722	0.242
Interpolated	144.3	4.09	0.723	0.356
F8.40	145.8	4.48	0.723	0.381
F7.20	138.9	3.71	0.662	0.197
Interpolated	140.1	4.20	0.686	0.212
F7.40	141.7	4.83	0.718	0.231
Average After Interpolation	142.2	4.15	0.705	0.284

Note: 1 pcf = 157.1 kN/m , 1 psi = 6.9 kPa

Table 6.2 Creep Compliance of Fine Asphalt Mixtures for Computer Input

Specimen No.	Density (pcf)	Creep Compliance (10^{-7} in. /lb) Loading Time (sec) 0.01	0.03	0.1	0.3	1.0	3.0	10	30	100	300	1000
F8.5	137.5	3.12	9.37	24.20	46.98	80.68	115.06	151.10	179.74	207.42	233.68	272.36
Interpolated	144.3	3.43	5.46	10.27	18.28	32.73	53.19	86.65	128.84	182.90	224.53	238.68
F8.40	145.8	3.50	4.61	7.25	12.05	22.32	39.76	72.66	117.79	177.57	222.55	231.37
F7.20	138.9	8.53	15.24	26.24	39.98	59.18	80.24	106.89	134.41	168.68	205.10	253.76
Interpolated	140.1	5.46	10.50	19.63	31.92	49.73	69.35	93.77	118.60	149.86	184.93	237.26
F7.40	141.7	1.53	4.44	11.19	21.63	37.67	55.45	77.02	98.43	125.83	159.19	216.20
Average of Centrifuge Specimen	142.2	4.44	7.98	16.95	25.10	41.23	61.27	90.21	123.72	166.38	204.73	237.97

Note: 1 in. = 25.4 mm, 1 lb = 4.45 N, 1 pcf = 157.1 N/m^3

Properties of Sand Subgrade

The properties of sand subgrade include the coefficients K_1 and K_2 for resilient modulus, the permanent deformation parameters,α and μ, under repeated loading, and the creep compliance under static loading. Because the cylindrical specimens were compacted to the same density as the sand subgrade in the centrifuge, the properties of cylindrical specimens presented in Chapter 5 were used directly with no interpolations needed. A Poisson's ratio of 0.3 was assumed for the sand subgrade.

6.2 Comparison of Results under Repeated Loading

The responses to be compared under repeated loading include the resilient surface deformation, the resilient tensile strain at the bottom of asphalt layer, the vertical permanent deformations at different repetitions, and the permanent deformation parameters α and μ. The computer solutions for the first two responses were obtained by KENLAYER and those for the last two by VESYS. The VESYS solutions also provided values of the first two responses, which were checked against the KENLAYER solutions and found in good agreement. One of the advantages of using KENLAYER is the availability of either bonded or unbonded interface, while only the bonded interface is available in VESYS.

Resilient Modulus of Sand Subgrade

There are two methods to input the resilient modulus of sand into a computer model. If the model is nonlinear, the coefficients K_1 and K_2 can be inputted and the resilient modulus determined by an iteration method based on the state of stresses until the modulus converges to a specified tolerance. If the model is linear, the resilient modulus must be obtained from the repeated load test, using the same level of stresses as in the pavement, and inputted directly into the computer.

Table 6.3 shows the stresses at the midheight of the sand layer and the

resulting resilient modulus as obtained by KENLAYER. The loading stresses were based on a contact pressure of 90 psi (621 kPa), which includes both the repeated load and the weight of LVDT plate. It can be seen that the total radial stresses average about 1 psi (7 kPa) and the vertical loading stress average about 3.6 psi (25 kPa). These values check reasonably well with the confining pressure of 1.16 psi (8 kPa) and the repeated stress of 3 psi (21 kPa) used in the repeated and static load tests of cylindrical sand specimen.

Table 6.3 Stresses in Sand Layer of Prototype Pavement

Loading Stress(psi)			Geostatic Stress(psi)			Total Stress(psi)			Resilient Modulus
Vertical	Radial	θ	Vertical	Radial	θ	Vertical	Radial	θ	(psi)
3.57	0.31	3.88	1.76	0.70	3.17	5.33	1.01	7.05	15,540

Note: 1 psi = 6.9 kPa

Resilient Deformations and Strains

After the resilient modulus of the sand subgrade had been determined, as described in the previous section, KENLAYER was run again as a linear layered system by inputting directly the resilient modulus as the elastic modulus of the sand subgrade. A load intensity of 80 psi (552 kPa) was used to simulate the repeated load.

Table 6.4 and Figure 6.1 show a comparison of vertical resilient deformations and radial resilient strains between the centrifuge models and the computer solutions. It can be seen that the computer solutions check very well with the centrifuge model in resilient deformations but not as well in resilient strains. However, the agreement is considered satisfactory in view of the variability of the measurements.

Table 6.4 Comparison of Resilient Deformation and Strain under Repeated Load

Response	Centrifuge (Overall)	KENLAYER (Bonded)	KENLAYER (Unbonded)
Deformation (10^{-3} in.)	6.80	5.74	6.38
Strain (10^{-6} in./in.)	184.3	124.9	140.0

Note: 1 in. = 25.4 mm

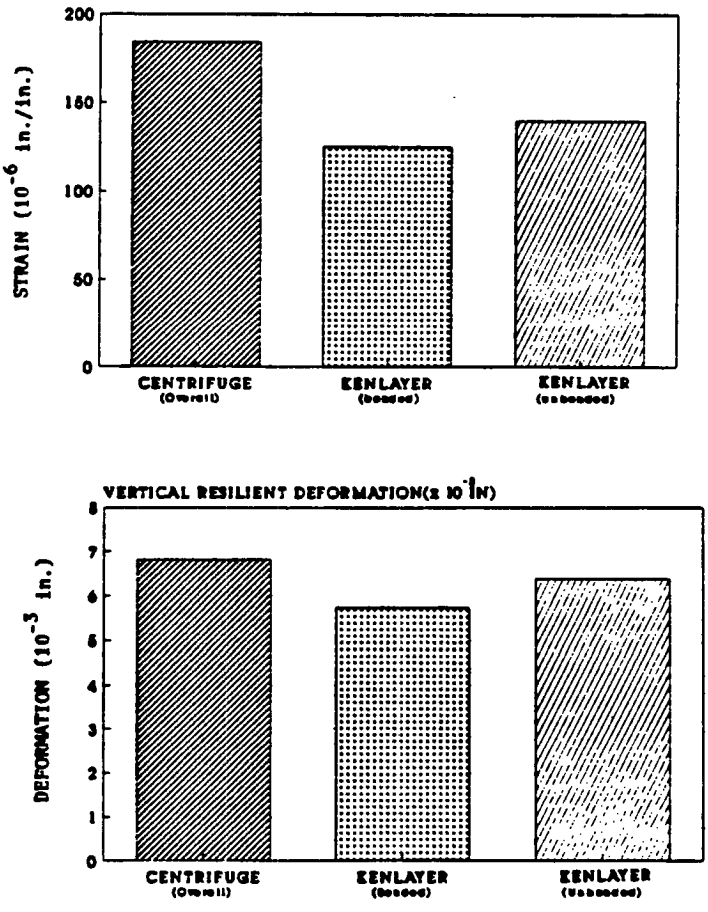

Figure 6.1 Comparison of resilient deformation and strain under repeated load (1 in. = 25.4 mm)

Permanent Deformations

The resilient modulus of sand obtained by KENLAYER, the resilient modulus of asphalt mixture, and the permanent deformation parameters, α and μ, of asphalt mixture and sand were inputted into VESYS to determine the permanent deformations at various number of repetitions as well as the permanent deformation parameters of the system, α and μ. The results are presented in Table 6.5 and plotted in Figure 6.2. As can be seen, the permanent

Table 6.5 Comparison of Permanent Deformations under Repeated Load

Response	Vertical Permant Deformation (10^{-3} in.)					α	μ
	Number of Repetitions						
	1	10	100	1000	10000		
Centrifuge	9.83	19.19	32.70	56.60	99.63	0.753	0.474
VESYS	3.64	7.82	15.61	30.72	60.30	0.707	0.160

Note: 1 in. = 25.4 mm

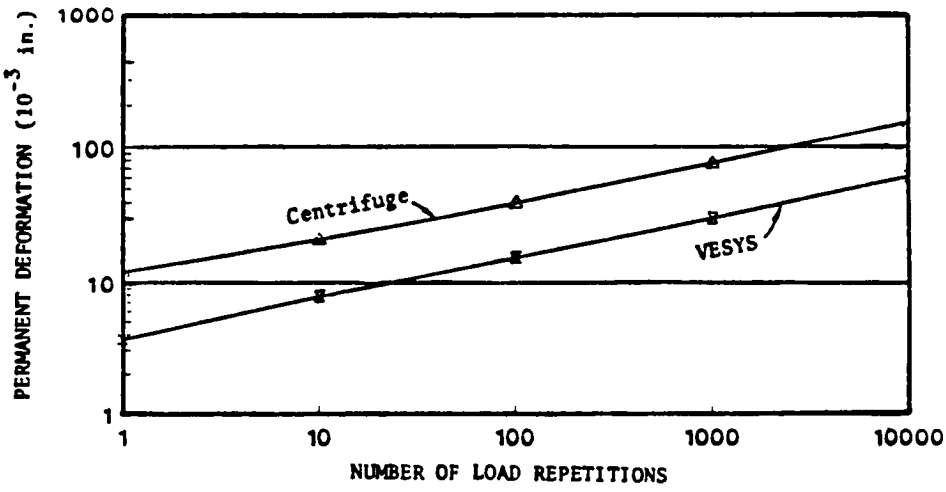

Figure 6.2 Comparison of p e rmanent deformations under repeated load (1 in. = 25.4 mm)

deformations obtained by VESYS are considerably smaller than those obtained from the centrifuge model but the slopes of the lines are nearly the same. The values of α checks pretty well but the values of μ obtained by VESYS are much smaller than those obtained from the centrifuge model, due to the smaller permanent deformations. It is believed that the much larger permanent deformations and the slightly larger resilient deformation and strain in centrifuge models are caused by the lack of intimate contact between the asphalt layer and the subgrade.

6.3 Comparison of Results under Static Loading

The results to be compared under static loading include the vertical surface deformations and the radial tensile strains at various loading times. The creep compliances of the asphalt layer and the sand subgrade were inputted into KENLAYER to determine the responses under a 90 psi (621 kPa) static load. Note that the creep compliance of sand was determined from cylindrical specimens using a confining pressure of 1.16 psi (8 kPa) and a deviator stress of 3 psi (21 kPa), which were similar to the level of stresses in the prototype pavement. Therefore, the sand can be considered as linear and the linear viscoelastic option can be used.

Surface Deformations

Table 6.6 is a comparison of vertical deformations on the pavement surface between the centrifuge models and the two cases of computer solutions, one based on the bonded interface and the other based on the unbonded interface. The results are plotted in Figure 6.3. It can be seen that the deformations of the centrifuge model are much larger than the computer solutions at short loading times but the differences become much smaller at long loading times.

Table 6.6 Comparison of Vertical Deformations under Static Load

Method	Deformation (10^{-3} in.)										
	Loading Time (sec)										
	0.01	0.03	0.1	0.3	1	3	10	30	100	300	1000
Centrifuge	2.47	4.55	8.36	12.90	17.79	21.18	23.46	24.74	26.14	28.31	33.29
KENLAYER Bonded	0.60 (4.12)	1.92 (2.37)	4.20 (1.99)	6.46 (2.00)	8.81 (2.02)	10.70 (1.98)	13.04 (1.80)	15.99 (1.55)	20.10 (1.30)	23.50 (1.20)	24.30 (1.37)
KENLAYER Unbonded	0.69 (3.56)	2.10 (2.17)	4.72 (1.77)	7.28 (1.77)	9.65 (1.84)	12.24 (1.73)	15.07 (1.56)	18.56 (1.33)	23.35 (1.12)	27.35 (1.04)	28.39 (1.17)

Note: Numbers in parenthesis are the ratio of centrifuge measurement to computer solution. 1 in. =25.4 mm

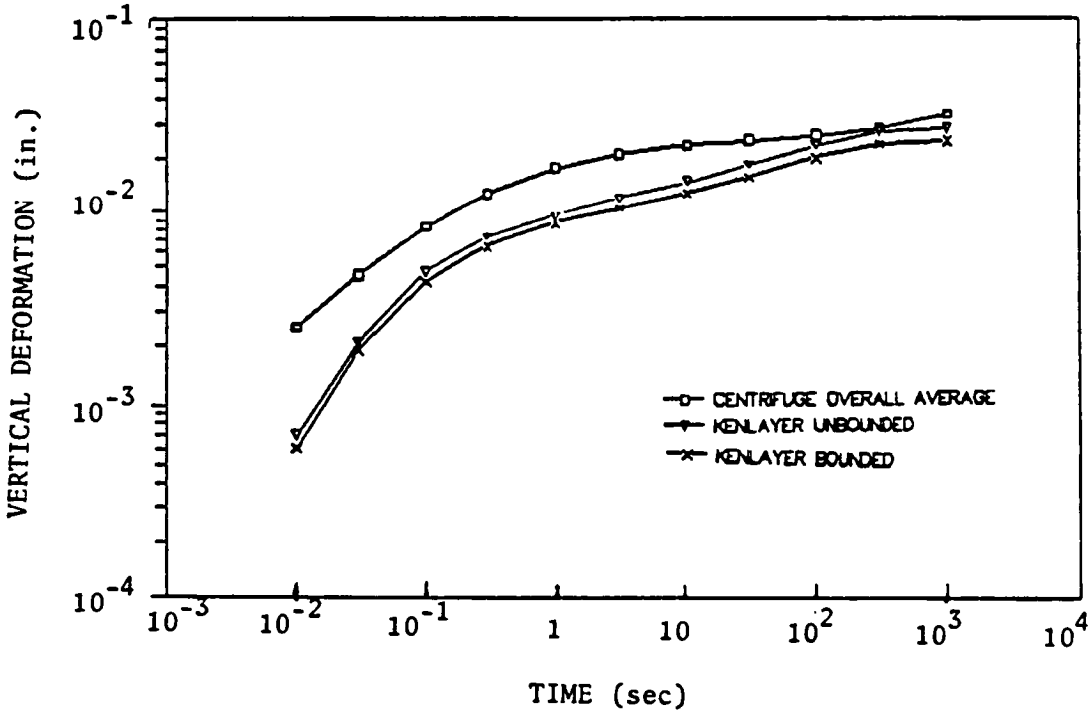

Figure 6.3 Comparison of vertical deformations under static load (1 in. = 25.4 mm)

Radial Strains

Table 6.7 is a comparison of radial strains at the bottom of asphalt layer. The results are plotted in Figure 6.4. Similar to the vertical

deformations, the radial strains obtained by the centrifuge model are much larger at short loading times.

Table 6.7 Comparison of Radial Strains under Static Load

Method	Strain (10^{-6} in./in.)										
	Loading Time (sec)										
	0.01	0.03	0.1	0.3	1	3	10	30	100	300	1,000
Centrifuge	78.1	143.3	241.8	344.4	450.6	527.7	585.7	619.9	649.6	683.7	748.7
KENLAYER Bonded	14.8 (5.28)	42.8 (3.35)	88.2 (2.74)	141.3 (2.44)	204.2 (2.21)	260.5 (2.03)	324.3 (1.81)	394.0 (1.57)	486.2 (1.34)	558.4 (1.22)	546.1 (1.37)
KENLAYER Unbonded	21.2 (3.68)	49.4 (2.90)	98.3 (2.46)	159.4 (2.16)	240.8 (1.87)	327.1 (1.61)	441.4 (1.33)	572.1 (1.08)	741.9 (0.88)	886.3 (0.77)	956.5 (0.78)

Note: Numbers in parenthesis are the ratio of centrifuge measurement to computer solution.

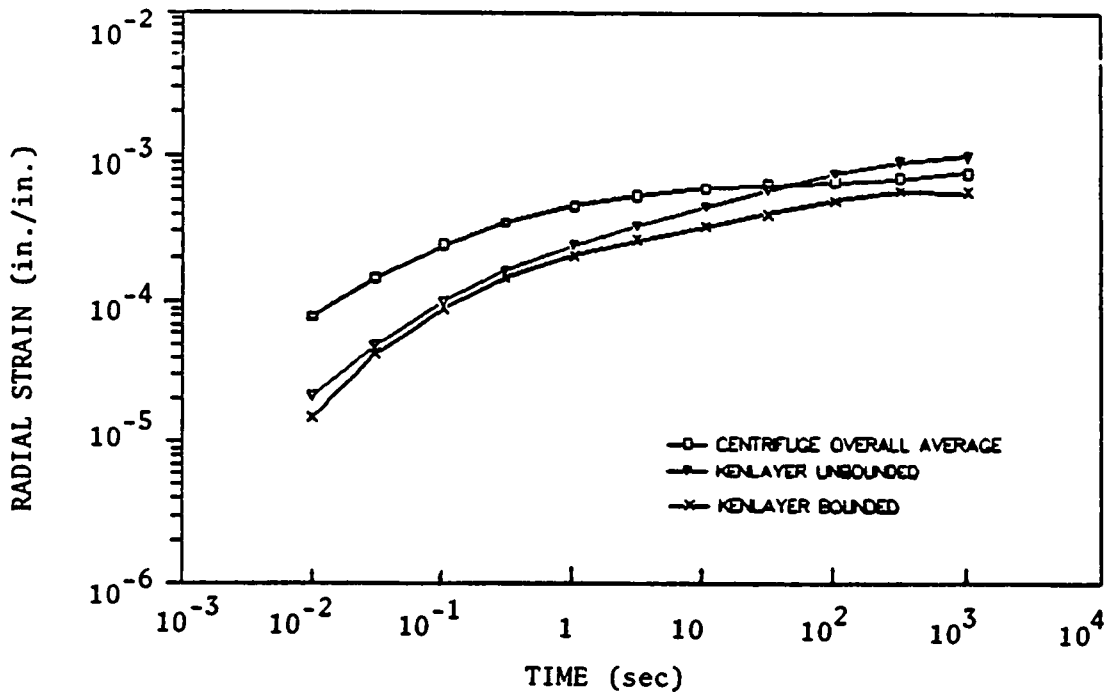

Figure 6.4 Comparison of radial strains under static load

Both the static and repeated load tests have indicated that the deformations and strains obtained by the centrifuge models are greater than those by the computer models. Other than the difference in contact conditions as explained previously, other factors may also contribute to the discrepany. For example, the computer models assume that each layer is homogeneous with the same elastic modulus throughout the layer, whereas the modulus of sand layer should decrease with increasing lateral distances from the load. The resilient modulus of asphalt layer for the computer models was obtained from tests on cylindrical specimens under a stress of 20 psi (138 kPa), which is small compared to an actual loading of 80 psi (552 kPa). If larger stresses were used in the tests, the resilient modulus of asphalt layer would decrease and a better match between the centrifuge and computer models obtained. The 20 psi (138 kPa) stress was recommended by the VESYS user's manual (FHWA, 1976) for both static and repeated load tests.

Chapter 7 Conclusions and Recommendations

As indicated in chapter 1, the main objective of this research was to investigate the possibility of predicting fatigue cracking and rutting in full depth asphalt pavements by centrifuge modeling. The major conclusions of this research are that centrifuge models can be used to predict pavement distresses and that the results obtained from the models check reasonably well with the computer solutions, in view of the variability of the tests. When the asphalt layer is prefabricated and placed on the surface of the subgrade, the asphalt layer and subgrade will not be in intimate contact. Although this contact problem can be alleviated partially by applying centrifugal forces, it still cannot be completely eliminated. This conclusion is supported by the facts that the resilient strains and deformations obtained by the 10g tests are slightly greater than those by the 20g tests, that the strains and deformations obtained by the 1g tests are several times greater than those by the 20g tests, and that the strains and deformations obtained by the model tests are greater than those by the computer programs based on full contact.

The use of small-scale pavement models subjected to centrifugal forces and repeated loads for predicting fatigue cracking and rutting is a new concept which has not been tried before anywhere in the world. This exploratory study has indicated the great promise of centrifuge testing for pavement analysis and design. However, the following improvements should be made before the model can be put into practical use:

1. Due to the small size of the centrifuge capsule, the existing model can only test a full depth sand asphalt on a subgrade of very limited depth with only two scale factors. A larger and longer capsule should be designed and constructed to accommodate thicker layers, larger aggregates for asphalt

concrete and granular base, and several different scale factors. More extensive tests can then be made to substantiate the modeling concept.

2. The existing loading mechanism is very crude and the loading waveform cannot be accurately controlled. Due to the tear and wear of the mechanism and the limit of testing time, only 10,000 repetitions were applied in the repeated load test and no fatigue cracking could be observed. A pneumatic or electrohydraulic loading system should be installed so that various waveforms with repetitions up to 1 million or more can be applied until the model fails.

3. The resilient deformation of the tape used to fasten the loading disk constituted a significant part of the total resilient deformation measured. The same was true for the permanent deformation of the tape at the initial stage when the total permanent deformation was small. Errors in the calibration of tape deformations may have a significant effect on the centrifuge results. It is preferable that the loading disk be fixed to the asphalt surface by other means rather than by the tape. The replacement of the loading disk by a flexible membrane with an internal device for measuring the deformation at the center of the loaded area is highly desirable because it can simulate more realistically the actual tire applied to the pavement surface.

4. It was assumed in this investigation that the base plate of the capsule was subjected to some resilient deformation but not to permanent deformations. The calibration of the resilient deformation for the base plate was based on many assumptions, which may induce some inaccuracy in the final results. It is recommended that a LVDT be mounted at the center of the base plate outside the capsule, so that both resilient and permanent deformations of the base plate can be monitored directly.

5. The present facility can test the small-scale models only at room temperature. It is recommended that the capsule be insulated and equipped with a temperature control device, so the responses of the model can be evaluated at different temperatures.

6. Further research is needed on the feasibility of compacting the asphalt mixture directly on the top of the subgrade to insure that the asphalt layer and the subgrade are in full contact. This procedure may cause

difficulties in installing a strain gage on the underside of the asphalt layer and in compacting the thin asphalt layer without disturbing the subgrade. If the centrifuge modeling concept is valid, it is really not necessary to monitor the tensile strains, a direct observation of fatigue cracking is a better approach than the measuring of tensile strains. To observe and measure the surface cracking within the capsule, some optical and electronic equipment will be needed.

With the above improvements, a comprehensive program of centrifuge tests can be implemented to find the effect of various factors on the fatigue cracking and permanent deformation of asphalt pavements. The advantage of centrifuge testing is that it gives directly the extent of fatigue cracking and rutting at any given number of load repetitions by considering not only the properties of each component layer but also the interaction between all layers. Extreme care should be taken in the preparation of small-scale models. A small weak spot may have only a small effect on the deformation of a prototype pavement but a large effect on that of a small-scale model after being scaled back to the prototype.

References

Cheney, J. A., 1982. Recent Advances in Geotechnical Centrifuge Modeling, Proceedings, University of California, Davis.

FHWA, 1978. Predictive Design Procedures, VESYS Users Manual, Report No. FHWA-RD-77-154, Federal Highway Administration.

Kenis, W. J., J. A. Sherwood and T. F. Memahan, 1982. Verification and Application of the VESYS Structural Subsystem, Federal Highway Administration.

Shell, 1978. Shell Pavement Design Manual, Asphalt Pavements and Overlays for Road traffic, Shell International Petroleum Company, London.

Huang, Y. H., 1969. "Finite Element Analysis of Nonlinear Soil Media," Proceedings, Symposium on Application of Finite Element Methods in Civil Engineering, Vanderbilt University, pp. 663-690.

Huang, Y. H., 1990. "Chapter 3 KENLAYER Computer Program," A manuscript on Pavement Analysis and Design to be published by Prentice Hall in 1992.

Roghani, M. H., 1990. Prediction of Pavement Responses by Small-Scale Centrifuge Models, Doctor's Dissertation, University of Kentucky, Lexington, Ky.

Seed, H. B., F. G. Mitry, C. L. Monismith, and C. K. Chan, 1965. Prediction of Pavement Deflections from Laboratory Repeated Load Tests, Report No. TE-65-6, Soil Mechanics and Bituminous Materials Research Laboratory, University of California, Berkeley.

TAI, 1979. Mix Design Methods for Asphalt Concrete and Other Hot-Mix Types, MS-2, The Asphalt Institute.

Timoshenko, S. and I. N. Goodier, 1951. Theory of Elasticity, McGraw-Hill.

Yoder, E. J. and M. W. Witczak, 1975. Principles of Pavement Design, John Wily and Sons.